공학석사학위논문

Analysis of Vibration and Radiated Noise of Circular Cylindrical Shell using Spectral Finite Element Method and Boundary Element Method

스펙트럴유한요소법과 경계요소법을 이용한

원통형 쉘의 구조진동 및 방사소음 해석

2009년 8월

서울대학교 대학원

조선해양공학과

이 영 구

공학석사학위논문

Analysis of Vibration and Radiated Noise of Circular Cylindrical Shell using Spectral Finite Element Method and Boundary Element Method

스펙트럴유한요소법과 경계요소법을 이용한

원통형 쉘의 구조진동 및 방사소음 해석

2009년 8월

서울대학교 대학원

조선해양공학과

이 영 구

Analysis of Vibration and Radiated Noise of Circular Cylindrical Shell using Spectral Finite Element Method and Boundary Element Method

지도교수 홍 석 윤

이 논문을 공학석사학위 논문으로 제출함

2009년 4월

서울대학교 대학원

조선해양공학과

이 영 구

이영구의 석사학위 논문을 인준함

2009년 6월

위 원 장 _____

부위원장 _____

위 원 _____

Analysis of Vibration and Radiated Noise of Circular Cylindrical Shell using Spectral Finite Element Method and Boundary Element Method

Abstract

The vibration characteristic of cylindrical shells is more difficult to analyze than those of plates because of 3-D coupling effects. Since it is difficult and complex to express the governing equations of motion of a cylindrical shell in exact form, many approximated forms of the governing equations have been presented based on reasonable assumptions. Based on Love's equation, the spectral finite element method (SFEM) is introduced to predict the frequency response function of finite circular cylindrical shells under simply supported – free boundary condition. In contrast to the FEM formulated in the time-domain and generally used in conjunction with the modal analysis method, the spectral finite element method (SFEM) is a frequency-domain solution method, in which the spectral element matrix formulated from the exact solutions of the governing differential equations are used in conjunction with the FFT-based spectral

analysis method. To verify the results from structural vibration analysis, which is formulated with the spectral finite element method, comparisons of the results with those of NASTRAN, which is FEM based commercial code, are carried out.

And for the radiated noise analysis of cylindrical shells, the boundary element method (BEM) is applied. The boundary element method is a numerical computation method used to solve linear partial differential equations that are formulated as integral equations. Specifically, the indirect boundary element method for a radiated noise analysis in open sound field is introduced and formulated using MATLAB program, with the out-of-plane displacements from structural vibration analysis as an input. And SYSNOISE, which is BEM based commercial code, is used to verify the radiated noise results. Finally, a full procedure that analyzes both structural vibration and radiated noise simultaneously is established.

Keywords: Circular Cylindrical Shell, Spectral Finite Element Method (SFEM), Boundary Element Method (BEM), Frequency Response Function (FRF), Structural Vibration Analysis, Radiated Noise Analysis

Student number: 2007-22941

Contents

Figures

Tables

1. Introduction

1.1. Research Motive and Objectives

Structural vibration and radiated noise analysis is a very important process in engineering design. In the case of submarines, structural vibration and radiated noise from the hull structure is directly connected to survival in battlefields. Similarly, structural vibration and radiated noise greatly affect the safety and comfort of passengers are on aircrafts and cruise liners for a long period of time. Therefore research and analysis on structural vibration and radiated noise has lately become a subject of special interest. In this paper, structural vibration and radiated noise analysis are carried out on a circular cylindrical shell, which is the simplest form of element in a curve-linear structure, before work is done on a more complex structure.

The governing equation of motion of cylindrical shell is more complex than those of a beam and plate because the radius of curvature and coupling effects on in-plane and out-of-plane waves need to be considered. Since it is difficult and complex to express the governing equation of motion of a cylindrical shell in exact form, many approximated forms of the governing equation have been

presented based on reasonable assumptions. Leissa [2] categorized and compared various shell theories. There are 9 different forms of the approximated governing equation of a circular cylindrical shell. The well(-) known ones are the Love-Timoshenko, Reissner-Naghdi-Berry, Flugge-Byrne-Lurye, and Sanders forms, etc. Among these, the approximated form of Love-Timoshenko is used in this study.

A famous analysis method for structural vibration is the finite element method (FEM). Although this method can be used for a wide range of applications, it has a critical weakness: FEM uses a static frequency-independent shape function. So when the frequency to be analyzed approaches the high-frequency range, it requires an exponential increase in operation time and costs. Therefore, incorrect results are obtained in the high-frequency range.

To overcome this problem, the Spectral Finite Element Method is suggested in this paper. In contrast to the FEM, which is formulated in the time-domain and generally used in conjunction with the modal analysis method, the spectral finite element method (SFEM) is a frequency-domain solution method, in which the spectral element matrix formulated from the exact solutions of the governing differential equations are used in conjunction with the FFT-based spectral analysis method. Since SFEM uses a dynamic frequency-dependent shape function, reliable results can be obtained, regardless of the frequency range

analyzed. And SFEM requires less element segmentation than FEM. Impedance changing points are the only points for element segmentation in SFEM, unlike in FEM; therefore, operation time for analysis is shortened, making SFEM more superior to FEM.

Boundary element method, which uses structural vibration results as inputs, is applied for radiated noise analysis. Boundary element method is a numerical computation method for solving linear partial differential equations formulated as integral equations. Largely, there are two kinds of BEM: indirect BEM and direct BEM. For radiated noise analysis of a cylindrical shell in an open sound field, indirect BEM is used with the out-of-plane displacement from structural vibration analysis as an input.

In this paper, structural vibration and radiated noise analysis of a circular cylindrical shell are carried out. And unlike most of researches that have analyzed structural vibration and radiated noise separately, a full procedure that analyzes both structural vibration and radiated noise simultaneously is established.

1.2. The State of Art

The vibration theory of a cylindrical shell has been studied extensively for more than 100 years. Because the boundary conditions significantly affect the

mode shapes and natural frequencies of vibration, the prediction of natural frequencies and mode shapes for different boundary conditions has been the main thrust in the study of finite length cylindrical shells. Wang [9] predicted the natural frequen-cies of finite length circular cylindrical shells for different boundary conditions using a novel wave approach. And attention also has been paid to the dispersion relation for wavenumbers in general. Sarkar [7] suggested an alternative derivation of the dispersion relation for the transverse vibration of a circular cylindrical shell. He found that the shallow shell theory model leads to a simpler derivation of the same results.

Because the equations of motion of cylindrical shells for relevant boundary conditions are more complex than those of beams and plates, it is very difficult to obtain an analytical solution to these equations. Numerous papers have proposed methods to establish and solve the equations effectively by invoking various assumptions. According to Leissa [2], who summarized and compared about 12 of these methods, all these methods invoked assumptions that simplify the equations of motion so that they can be solved analytically for different boundary conditions. Obviously, because approximate equations of motion were used, the relationships derived for the natural frequencies and wave numbers, the modal wave numbers and the mode shapes gave all approximated solutions, which only apply under specific conditions. Donnell's equation [3] provides good results only

for very thin and long circular cylindrical shells, and the equation developed by Lord Rayleigh [4], is only valid for high order vibration modes of circular cylindrical shells, etc.

On the other side, various methods have been applied to analyze the free vibration of cylindrical shells. Xuebin [5] presented a wave propagation approach for the free vibration analysis of circular cylindrical shells, based on the *Flügge* classical thin shell theory. The validity and accuracy of the wave propagation approach was studied in detail, including the aspects of frequencies, vibration shapes and wavenumbers. Zhang [6] also used the wave propagation approach method for vibration analysis of cylindrical shells. And he compared the results with those of the numerical finite element method. In recent years, some researchers have used the finite element method to analyze the vibration behavior of finite length cylindrical shells. However, this method is tedious for exploring the influence of all the parameters on the vibration behavior of the shells.

For engineering applications and acoustic analysis, an approximate analytical solution may provide more insight into the vibration behavior of finite length cylindrical shells, provided that the solution can satisfy certain predetermined criteria.

In this paper, unlike most of the researches and papers that FEM analysis, the vibration analysis of circular cylindrical shells is carried out by using the spectral

element method. A part of the present research was already investigated by Doyle [8] fairly restrictively with respect to boundary conditions and dispersion relations for wavenumbers. He suggested wavenumbers for very high analysis frequency and did not consider any external forces and boundary conditions. Therefore, based on wavenumbers, which are calculated from the spectrum relation of the governing equation of motion, the spectral finite element method can be applied effectively in the vibration analysis of circular cylindrical shells for simply-supported and free boundary conditions

2. Spectral Finite Element Method

2.1. Introduction

Interpretation of the dynamic behavior of a structure has become important in engineering. And for structural vibration analysis, finite element method (FEM) is widely used and more so, with the advancement of computer technology. Since FEM computes at the elemental level, the structure to be analyzed has to be segmented into elements. But increasing the number of elements leads to additional computational burden. However, this computation burden has been overcome by developments in computer technology. FEM provides convenient analysis of any shapes of complex structures without knowledge of the structure's analytical (exact) solution; this is FEM's strong point. But there are also shortcomings of FEM. Since FEM uses frequency independent static shape function, it is hard to predict a response of a structure in the high-frequency range. In the high frequency range, FEM shows a numerical error, but this error can be reduced by using a finer mesh. To make a finer mesh, more segmentation is needed. But excessive element segmentation leads to unmanageable computational burden and can cause local mode error.

In this aspect, the spectral finite element method is an adequate compensating method having many advantages that the FEM doesn't have. SFEM is a terminology that comes from the combination of spectral element method (SEM) and finite element method (FEM). (See Fig. 2.1) SFEM uses a frequency dependent dynamic shape function. So, element segmentation is not necessary even when analysis frequency increases into the high-frequency range. Selective segmentation is the big difference between SFEM and FEM. In the case of SFEM, element segmentation is required only at the points which have different mechanical impedances. In other words, impedance changing points where external force is applied or material property is changed are the only parts that need segmentation. Because of this feature, SFEM can give a reasonable solution independent of the analysis frequency range. And it carries out analyses very fast at high frequency, much faster than FEM at the same conditions.

To formulate SFEM, the governing equations of motion of structures are considered. This can be an advantage or disadvantage. Solution from SFEM is almost the same as the exact solution because the spectral element matrix is formulated using governing equations; this is the advantage. But when the governing equation is unknown due to the complexity of the structure, SFEM formulation is impossible; this is the disadvantage in comparison to FEM, which can formulate any type of structure. All these features are presented in Table. 2-1.

SFEM is carried out in the frequency domain. Fig. 2.2 shows the basic process of SFEM step by step. As mentioned above, the governing equation of motion is essential in obtaining the spectrum relation equation. In addition, the wave-numbers are required to produce the frequency dependent exponential shape function. It can be obtained from the dispersion relation equation, which comes from the determinant of the spectrum relation matrix. Using the spectrum relation and wavenumbers calculated, the spectral element matrix can be obtained. Since the spectral element matrix is already expressed in the frequency domain, the external force from the time to the frequency domain should be transformed. Use of DFT (Discrete Fourier Transform) is effective. From this whole process, the frequency response function (FRF) can be obtained as the final result.

There are quite often situations to which the SFEM can be most efficiently applied. They may include the followings:

(1) When it is significantly easier to measure the constitutive equation (including the frequency-dependent viscoelastic damping) of a material in the frequency domain rather than in the time domain.

(2) When the frequency dependent spectral element model is available for a structure.

(3) When the external forces are so complicated that one has to use the numerical integration to obtain the dynamic responses by using the excitation values at a discrete set of instants.

(4) When the modern data acquisition systems are used, as in most experimental measurements, to store digitized data through the analogue to digital converts.

2.2. Spectral Formulation

2.2.1. Introduction

When the structural vibration of a structure is analyzed by the spectral finite element method, it is essential and important to derive the spectral element matrix. To do this, the governing equation of motion of the structure should be obtained first. For general and common structures in engineering fields like beams and plates, the governing equations of motion have been established. So, in this section, the derivation of governing equations of motion is not carried out.

Three spectral formulations shown below are assumed to be the bases of SFEM for the investigation of circular cylindrical shells. Spectral formulation of beams is a important, basic one dimensional problem. Depending on the assumptions, beams are separated into two categories: the Euler beam and the Timoshenko beam. Spectral formulation is carried out for both categories. And for two dimensional spaces, the Kirchhoff plate with the simply supported boundary condition is formulated.

Spectral formulation is also performed on more complex structures, which are briefly described below (for more details, refer to [14] and [16]).

Sung Ju Lee [16] presented applications of SFEM for the rectangular Levy's

type sandwich plate. The applied sandwich plate consists of three bonded layers: a viscoelastic plate inserted between two elastic plates. The in-plane and transverse motion were analyzed for the elastic plates and only the shear motion for viscoelastic plate. And the frequency dependent complex shear modulus of the viscoelastic plate is reflected in the analysis by the Golla-Hughes-McTavish (GHM) method. The results of the frequency response function and dynamic response of the sandwich plate are presented.

Jee Hun Song [14] developed spectral finite element models for the passive constrained layer damping (PCLD) beam and plate considering the frequency dependent stiffness and damping properties of viscoelastic materials. The results of the frequency response function and dynamic responses for PCLD beam and plate were presented and validated by experimental results and other analyses; including the assumed modes method (AHM) and the conventional finite element method (CFEM). Using the developed theories, the floating floor software program is also developed by him to predict the structure-borne noise in ship cabins. The predicted results of the structure-borne noise from the use of a floating floor are compared to the measurements of a mock-up. Various floating floor structures are studied, and the effects of the variations of thickness, density, and stiffness of the high-density mineral wool are investigated.

2.2.2. Euler Beam

To obtain the spectral element matrix, the governing equation of motion should be considered first, which derives the spectrum relation for the Euler beam and is presented as

$$\rho A\ddot{\omega} + \frac{\partial^2}{\partial x^2}\left[EI\left(\frac{\partial^2 w}{\partial x^2} \right) \right] = q \,, \tag{2.1}$$

where ρ is density, A is cross-sectional area, ω is frequency, E is Young's modulus, I is moment of inertia, and q is external force. Originally, the spectrum relation can be obtained from free vibration equation of motion. When external force is zero, q=0, equation (2.1) represents motion of free vibration.

Displacement solution is assumed as sum of time harmonic exponential functions based on the Fourier series in the form:

$$w(x,t) = \sum_{n=1}^{\infty} W_n(x) \cdot e^{iwt} \,, \tag{2.2}$$

where $W_n(x)$ is the Fourier coefficient, ω is angular frequency. After substituting equation (2.2) for w in equation (2.1), we can obtain

$$\sum_{n=1}^{\infty}\left(-\rho A\omega^2 W_n(x)+EIW_n''''(x)\right)\cdot e^{iwt}=0\ . \tag{2.3}$$

From orthogonality of harmonic function for all n, equations in a parenthesis of equation (2.3) should be zero. That is presented as

$$-\rho A\omega^2 W_n(x)+EIW_n''''(x)=0\ . \tag{2.4}$$

Equation (2.4) is a 4th order ordinary differential equation. And we make it simple form of equation as

$$W_n''''-k^4 W_n=0\ , \tag{2.5}$$

where

$$k^4=\frac{\rho A\omega^2}{EI}\ . \tag{2.6}$$

This is a dispersion relation equation. Particle velocity is defined from equation (2.6) as

$$c^2=\left(\frac{\omega}{k}\right)^2=\omega\sqrt{\frac{EI}{\rho A}}\ . \tag{2.7}$$

The particle velocity is a dependent function of angular frequency and increases with it. So, arbitrary waves propagate in beam have a characteristic that components of wave move slow for low frequency and fast for high frequency. Therefore, waves spread out with frequency. That is why equation (2.6) is called equation of dispersion relation.

General solution of equation (2.5) can be presented with wave numbers which are calculated in equation (2.6) as

$$W_n(x) = A_1 e^{-ikx} + A_2 e^{-kx} + A_3 e^{ikx} + A_4 e^{kx}. \tag{2.8}$$

As mentioned in previous section, the SFEM includes finite element concept in formulation. So, it is essential to consider element segmentation and node at separation points. Two node points exist in one element. The displacement and its derivative with longitudinal axis 'x' at each node are presented as follow:

$$w_1 = W(0) = A_1 + A_2 + A_3 + A_4,$$

$$\theta_1 = \frac{dW(x)}{dx}_{x=0} = A_1(-ik) + A_2(-k) + A_3(ik) + A_4(k),$$

$$w_2 = W(L) = A_1 e^{-ikL} + A_2 e^{-kL} + A_3 e^{ikL} + A_4 e^{kL}$$

and

$$\theta_2 = \frac{dW(x)}{dx}_{x=L} = A_1(-ik)e^{-ikL} + A_2(-k)e^{-kL} + A_3(ik)e^{ikL} + A_4(k)e^{kL}. \tag{2.9}$$

It is important to follow the standard sign rule for sign of displacements and forces at nodes throughout global coordinates. Matrix form of equation (2.9) is shown as

$$\begin{aligned}[W] &= \begin{bmatrix} w_1 \\ \theta_1 \\ w_2 \\ \theta_2 \end{bmatrix} = \begin{bmatrix} 1 & 1 & 1 & 1 \\ -ik & -k & ik & k \\ e^{-ikL} & e^{-kL} & e^{ikL} & e^{kL} \\ -ike^{-ikL} & -ke^{-kL} & ike^{ikL} & ke^{kL} \end{bmatrix} \begin{bmatrix} A_1 \\ A_2 \\ A_3 \\ A_4 \end{bmatrix} \\ &= [H(\omega)][A], \end{aligned} \tag{2.10}$$

where $[H(\omega)]$ is a matrix that shows relation between node displacement and amplitude of general displacement. This is a similar notation with shape function in the FEM.

Nodal force is indicated as

$$\begin{aligned} V_1 = V(0) &= -EI \frac{d^3W(x)}{dx^3}_{x=0} \\ &= -EI\left[A_1(ik^3) + A_2(-k^3) + A_3(-ik^3) + A_4(k^3)\right], \end{aligned}$$

$$M_1 = M(0) = -EI\frac{d^2W(x)}{dx^2}_{x=0}$$
$$= -EI\left[A_1(-k^2) + A_2(k^2) + A_3(-k^2) + A_4(k^2)\right],$$
$$V_2 = -V(L) = EI\frac{d^3W(x)}{dx^3}_{x=L}$$
$$= EI\left[A_1(ik^3)e^{-ikL} + A_2(-k^3)e^{-kL} + A_3(-ik^3)e^{ikL} + A_4(k^3)e^{kL}\right]$$

and

$$M_2 = -M(L) = EI\frac{d^2W(x)}{dx^2}_{x=L}$$
$$= EI\left[A_1(-k^2)e^{-ikL} + A_2(k^2)e^{-kL} + A_3(-k^2)e^{ikL} + A_4(k^2)e^{kL}\right]. \quad (2.11)$$

Equation (2.11) can be expressed in matrix form as

$$\left[F\right] = \begin{bmatrix} V_1 \\ M_1 \\ \mathrm{V}_2 \\ \mathrm{M}_2 \end{bmatrix} = EI\begin{bmatrix} -ik^3 & k^3 & ik^3 & -k^3 \\ k^2 & -k^2 & k^2 & -k^2 \\ ik^3e^{-ikL} & k^3e^{-kL} & -ik^3e^{ikL} & k^3e^{kL} \\ -k^2e^{-ikL} & k^2e^{-kL} & -k^2e^{ikL} & k^2e^{kL} \end{bmatrix}\begin{bmatrix} A_1 \\ A_2 \\ A_3 \\ A_4 \end{bmatrix} \quad (2.12)$$
$$= \left[G(\omega)\right]\left[A\right],$$

where $\left[G(\omega)\right]$ is a matrix that shows relation between the nodal force and amplitude of the general displacement. Using equation (2.11) and (2.12), the spectral element matrix is finally obtained as

$$\begin{bmatrix} V_1 \\ M_1 \\ V_2 \\ M_2 \end{bmatrix} = [G(\omega)][H(\omega)]^{-1} \begin{bmatrix} w_1 \\ \theta_1 \\ w_2 \\ \theta_2 \end{bmatrix} = [S(\omega)] \begin{bmatrix} w_1 \\ \theta_1 \\ w_2 \\ \theta_2 \end{bmatrix}, \tag{2.13}$$

where $[S(\omega)]$ is the spectral element matrix. This equation (2.13) is a simple form of the spectral formulation with only one element when no external force is applied between two nodes. There are two important factors in determination of displacement solution. One is boundary condition and the other is amplitude of external force. And when the number of element is more than one, local spectral element matrix in the form of equation (2.13) should be assembled to get global spectral element matrix.

2.2.3. Timoshenko Beam

In the discussions of the Euler beam at previous section, the effect from shear deformation is neglected in equation of motion. But in the case of beam is thick and have short length in longitudinal direction, effect of shear deformation should be considered. That is why Timoshenko beam model is suggested. This model includes the effect of shear deformation in equation of motion. (See Fig. 2.4)

Bending moment and shear force of beam are presented as

$$V_s = kGA[w' - \psi] \quad \text{and} \quad M = EI\psi', \tag{2.14}$$

where G is shear modulus, A cross-sectional area, E is young's modulus, I is moment of area, w is transverse displacement, ψ is rotation caused by bending. Assume a solution as

$$w(x,t) = \sum_{n=0}^{\infty} W_n(x) e^{i\omega_n t} \quad \text{and} \quad \psi(x,t) = \sum_{n=0}^{\infty} \Psi_n(x) e^{i\omega_n t}, \tag{2.15}$$

where

$$W(x) = \sum_{p=0}^{m} a_p e^{-ik_p x} \quad \text{and} \quad \Psi(x) = \sum_{p=0}^{m} r_p a_p e^{-ik_p x}, \tag{2.16}$$

m is the number of solution of characteristic equation, and r_p is a variable that represents ratio of two amplitude of waves in equation (2.15).

Usual procedure to obtain the spectrum relation starts from substitution of assumed solution into the governing equation. The governing equation of the Timoshenko beam is derived using the Euler-Lagrange equation as

$$-\frac{\partial}{\partial t}(\rho A \dot{\omega}) + \frac{\partial}{\partial x}\left[kGA\left(\frac{\partial w}{\partial x} - \psi \right) \right] + q = 0$$

and (2.17)

$$-\frac{\partial}{\partial t}(\rho I\dot{\psi})+\frac{\partial}{\partial x}\left(EI\frac{\partial \psi}{\partial x}\right)+kGA\left(\frac{\partial w}{\partial x}-\psi\right)=0\,,$$

where q is external vertical force. Since variable E, I, G, and A are supposed to be constants, equation (2.17) becomes a simple form of equation:

$$\rho A\ddot{w}-kGA(w_{xx}-\psi_x)-q=0$$

and (2.18)

$$\rho I\ddot{\psi}-EI\psi_{xx}-kGA(w_x-\psi)=0\,.$$

Then, put equation (2.15) into the governing equation (2.18) for the spectrum relation. This is shown as

$$\begin{bmatrix} kGAk_p^2-\rho A\omega^2 & -ik_pkGA \\ ik_pkGA & EIk_p^2+kGA-\rho I\omega^2 \end{bmatrix}\begin{Bmatrix} a_p \\ r_pa_p \end{Bmatrix}=\begin{Bmatrix}0\\0\end{Bmatrix}. \qquad (2.19)$$

To have solutions in equation (2.19), determinant of matrix on left hand side should be zero. Then, the characteristic equation and the dispersion relation equation is derived as

$$k_p^4 - \eta k_F^4 k_p^2 - k_F^4 (1 - \eta_1 k_G^4) = 0 \qquad p = 1,2,3,4 \tag{2.20}$$

where

$$k_F = \sqrt{\omega}\left(\frac{\rho A}{EI}\right)^{\frac{1}{4}},\ k_G = \sqrt{\omega}\left(\frac{\rho A}{kGA}\right)^{\frac{1}{4}}, \tag{2.21}$$

$$\eta_1 = \frac{I}{A},\ \eta_2 = \frac{EI}{kGA},\ \eta = \eta_1 + \eta_2 \tag{2.22}$$

and k_F is wavenumber for bending waves. And it is same with the wavenumber for waves in the Euler beam (See equation (2.6)). k_G is wavenumber for shear waves. Solution of equation (2.20) is calculated as

$$\begin{aligned}
k_1 &= \frac{1}{\sqrt{2}} k_p \sqrt{\eta k_F^2 + \sqrt{\eta^2 k_F^4 + 4(1 - \eta_1 k_G^4)}}, \\
k_2 &= \frac{1}{\sqrt{2}} k_p \sqrt{\eta k_F^2 - \sqrt{\eta^2 k_F^4 + 4(1 - \eta_1 k_G^4)}}, \\
k_3 &= -k_1 = -\frac{1}{\sqrt{2}} k_p \sqrt{\eta k_F^2 + \sqrt{\eta^2 k_F^4 + 4(1 - \eta_1 k_G^4)}}
\end{aligned} \tag{2.23}$$

and

$$k_4 = -k_2 = -\frac{1}{\sqrt{2}} k_p \sqrt{\eta k_F^2 - \sqrt{\eta^2 k_F^4 + 4(1 - \eta_1 k_G^4)}}\ .$$

And from equation (2.19), wave mode ratio (r_p) can be obtained as

$$r_p = \frac{1}{ik_p}\left(k_p^2 - \omega^2 \frac{\rho A}{kGA}\right) = \frac{1}{ik_p}(k_p^2 - k_G^2) \quad . \qquad (2.24)$$
$$p = 1,2,3,4$$

Therefore, it is possible to express the general solution based on the wave-numbers and wave mode ratio those are calculated above:

$$\begin{aligned} W(x) &= a_1 e^{-ik_1 x} + a_2 e^{+ik_1 x} + a_3 e^{-ik_2 x} + a_4 e^{+ik_2 x} \\ &= \left[e^{-ik_1 x} \quad e^{+ik_1 x} \quad e^{-ik_2 x} \quad e^{+ik_2 x}\right]\{a_1 \quad a_2 \quad a_3 \quad a_4\}^T \\ &= \Phi_w(x) A \end{aligned}$$

and (2.25)

$$\begin{aligned} \Psi(x) &= r_1 a_1 e^{-ik_1 x} + r_2 a_2 e^{+ik_1 x} + r_3 a_3 e^{-ik_2 x} + r_4 a_4 e^{+ik_2 x} \\ &= \left[r_1 e^{-ik_1 x} \quad r_2 e^{+ik_1 x} \quad r_3 e^{-ik_2 x} \quad r_4 e^{+ik_2 x}\right]\{a_1 \quad a_2 \quad a_3 \quad a_4\}^T \\ &= \Phi_\psi(x) A. \end{aligned}$$

For the spectral element matrix, it is essential to define the nodal displacements and spectral coefficients which have the same role with shape function in FEM. Simple form of it can be presented as

$$
\begin{aligned}
d &= \{W_1 \quad \Psi_1 \quad W_2 \quad \Psi_2\}^T \\
&= \{W(0) \quad \Psi(0) \quad W(L) \quad \Psi(L)\}^T \\
&= \begin{bmatrix} \Phi_w(0) \\ \Phi_\psi(0) \\ \Phi_w(L) \\ \Phi_\psi(L) \end{bmatrix} A = \begin{bmatrix} 1 & 1 & 1 & 1 \\ r_1 & -r_1 & r_2 & -r_2 \\ e^{-ik_1L} & e^{ik_1L} & e^{-ik_2L} & e^{ik_2L} \\ r_1 e^{-ik_1L} & -r_1 e^{ik_1L} & r_2 e^{-ik_2L} & -r_2 e^{ik_2L} \end{bmatrix} A \\
&= H_T(\omega) A,
\end{aligned}
\tag{2.26}
$$

where L is length between nodes.

Nodal force can be expressed as

$$
f_c = \begin{Bmatrix} Q_1 \\ M_1 \\ Q_2 \\ M_2 \end{Bmatrix} = \begin{Bmatrix} -Q(0) \\ -M(0) \\ +Q(L) \\ +M(L) \end{Bmatrix} , \tag{2.27}
$$

where Q is vertical force and M is bending moment at the node. Put equation (2.14) into equation (2.27) to have a detailed expression for nodal forces. Then, nodal forces are presented as

$$f_c = \begin{Bmatrix} -kGA[\Phi_w'(0) - \Phi_\psi(0)] \\ -EI\Phi_\psi'(0) \\ +kGA[[\Phi_w'(L) - \Phi_\psi(L)] \\ +EI\Phi_\psi'(L) \end{Bmatrix} = G_T(\omega)A, \tag{2.28}$$

where

$$G_T(\omega) = kGA\begin{bmatrix} +(ik_1 + r_1) & -(ik_1 + r_1) \\ +i\eta_2 k_1 r_1 & +i\eta_2 k_1 r_1 \\ -(ik_1 + r_1)e^{-ik_1 L} & +(ik_1 + r_1)e^{ik_1 L} \\ -i\eta_2 k_1 r_1 e^{-ik_1 L} & -i\eta_2 k_1 r_1 e^{ik_1 L} \\ +(ik_2 + r_2) & -(ik_2 + r_2) \\ +i\eta_2 k_2 r_2 & +i\eta_2 k_2 r_2 \\ -(ik_2 + r_2)e^{-ik_2 L} & +(ik_2 + r_2)e^{ik_2 L} \\ -i\eta_2 k_2 r_2 e^{-ik_2 L} & -i\eta_2 k_2 r_2 e^{ik_2 L} \end{bmatrix}. \tag{2.29}$$

To express nodal forces with nodal displacements, elimination of A in equation (2.28) is required. From equation (2.26), it is obvious that A is same with $H_T^{-1}(\omega)d$ .By putting this into equation (2.28), final form of equation is obtained:

$$f_c = G_T(\omega)H_T^{-1}(\omega)d = S_T(\omega)d\,, \tag{2.30}$$

where $S_T(\omega)$ is the spectral element matrix that is essential to formulate with

spectral finite element method (SFEM).

2.2.4. Kirchhoff Plate

Unlike beams (Euler or Timoshenko), derivation of the governing equation of plate is more complex than one dimensional structure for dynamic responses. And it is very important to study on structural vibration of plate since plate shows fundamental characteristics of 2 dimensional structures.

In the process of analysis with the SFEM, Levy's type boundary condition should be assumed first to derive the dispersion relation equation that consists of wave-number and frequency. So, plate model has boundary conditions of simply supported at parallel line y=0 and y=b and of arbitrary at parallel line x=0 and x=a. (See Fig. 2.5)

Based on time harmonic assumption, solution can be represented as multi-plication of frequency dependent complex exponential function in x-direction and series solution in y-direction. Series solution is a type of sine function that satisfies simply supported boundary condition. Solution is shown as

$$w(x,y,t) = W_x(x)W_y(y)e^{i\omega t} = \sum_{n=1}^{N}\left(Ae^{kx}\right)\left(\sin\frac{n\pi y}{b}\right)e^{i\omega t}, \qquad (2.31)$$

where n is mode number. The dispersion relation comes from the governing equation of motion of plate. So, it is essential to know that the governing equation before mentioning about any details of dispersion relation. The governing equation of motion is indicated as

$$D\left(\frac{\partial^4 w}{\partial x^4}+2\frac{\partial^4 w}{\partial x^2\partial y^2}+\frac{\partial^4 w}{\partial y^4}\right)+\rho h\frac{\partial^2 w}{\partial t^2}=f(x,y,t)\,, \qquad (2.32)$$

where D is a bending stiffness, w is vertical displacement, ρ is density, h is thickness, and f is external force. And when external force is zero ($f=0$), plate behavior shows characteristic of free vibration of motion as

$$D\left(\frac{\partial^4 w}{\partial x^4}+2\frac{\partial^4 w}{\partial x^2\partial y^2}+\frac{\partial^4 w}{\partial y^4}\right)+\rho h\frac{\partial^2 w}{\partial t^2}=0\,. \qquad (2.33)$$

As already indicated in equation (2.32) and (2.33), only out-of-plane wave component w will be discussed in this section because external forces are imposed in the direction of vertical to the plate. And since there is no coupling effect between in-plane and out-of-plane wave, separate use of one of those wave is possible. Substitution of equation (2.31) into (2.33) will show the dispersion

relation equation as

$$k^4 - 2\left(\frac{n\pi}{b}\right)^2 k^2 + \left(\left(\frac{n\pi}{b}\right)^4 - \frac{\rho h \omega^2}{D}\right) = 0. \qquad (2.34)$$

Wavenumbers as solutions of a 4th order dispersion relation equation (equation (2.34)) are obtained as

$$k_1 = +\sqrt{\left(\frac{n\pi}{a}\right)^2 + \omega\sqrt{\frac{\rho h}{D}}},$$
$$k_2 = -\sqrt{\left(\frac{n\pi}{a}\right)^2 + \omega\sqrt{\frac{\rho h}{D}}},$$
$$k_3 = +\sqrt{\left(\frac{n\pi}{a}\right)^2 - \omega\sqrt{\frac{\rho h}{D}}}$$

And (2.35)

$$k_4 = -\sqrt{\left(\frac{n\pi}{a}\right)^2 - \omega\sqrt{\frac{\rho h}{D}}}.$$

Using wavenumbers obtained above, x-directional solution component can be expressed as

$$W_x(x) = A_1 e^{k_1 x} + A_2 e^{k_2 x} + A_3 e^{k_3 x} + A_4 e^{k_4 x} . \qquad (2.36)$$

And it is necessary to introduce nodal displacements and its gradient using equation (2.36) at the two node in x-direction, x=0 and x=a. From now on, $W_x(x)$ is expressed with simplified form of notation W. Those is presented as

$$\begin{aligned} W_1 &= A_1 + A_2 + A_3 + A_4 , \\ \theta_1 &= A_1 k_1 + A_2 k_2 + A_3 k_3 + A_4 k_4 , \\ W_2 &= A_1 e^{k_1 a} + A_2 e^{k_2 a} + A_3 e^{k_3 a} + A_4 e^{k_4 a} \end{aligned} \qquad (2.37)$$

and

$$\theta_2 = A_1 k_1 e^{k_1 a} + A_2 k_2 e^{k_2 a} + A_3 k_3 e^{k_3 a} + A_4 k_4 e^{k_4 a} ,$$

where

$$W(0) = W_1 , \ \frac{\partial W}{\partial x}(0) = \theta_1 , \ \ W(a) = W_2 \ \ and \ \ \frac{\partial W}{\partial x}(a) = \theta_2 . \qquad (2.38)$$

Matrix form of equation makes calculation convenient and easy. So, transform equation (2.37) to matrix form as indicated below:

$$\begin{bmatrix} W_1 \\ \theta_1 \\ W_2 \\ \theta_2 \end{bmatrix} = \begin{bmatrix} 1 & 1 & 1 & 1 \\ k_1 & k_2 & k_3 & k_4 \\ e^{k_1 a} & e^{k_2 a} & e^{k_3 a} & e^{k_4 a} \\ k_1 e^{k_1 a} & k_2 e^{k_2 a} & k_3 e^{k_3 a} & k_4 e^{k_4 a} \end{bmatrix} \begin{bmatrix} A_1 \\ A_2 \\ A_3 \\ A_4 \end{bmatrix} \tag{2.39}$$
$$\approx [d] = [H(\omega)][A].$$

Force is the counterpart of displacement for spectral formulation. Two degrees of freedom are given at each node, one is bending moment and the other is shear force. These forces are presented as

$$M_x = -D\left(\frac{\partial^2 w}{\partial x^2} + \nu \frac{\partial^2 w}{\partial y^2}\right) \tag{2.40}$$

and

$$V_x = -D\left(\frac{\partial^3 w}{\partial x^3} + (2-\nu)\frac{\partial^3 w}{\partial x \partial y^2}\right). \tag{2.41}$$

General solution is obtained by substituting equation (2.36) for $W_x(x)$ in assumed solution equation (2.31), it is shown as

$$w(x,y) = \sum_{n=1}^{N}\left(A_1 e^{k_1 x} + A_2 e^{k_2 x} + A_3 e^{k_3 x} + A_4 e^{k_4 x}\right)\left(\sin\frac{n\pi y}{b}\right), \tag{2.42}$$

where time dependent term is neglected to make it simple and easy.

By putting this general solution to bending moment and shear force (equation (2.40) and equation (2.41)), forces are shown in detailed expressions as

$$M_x = -D\sum_{n=1}^{N}\left[\Phi_2 - \nu\, k_n \Phi_0\right]\left(\sin k_n y\right)$$

and (2.43)

$$V_x = -D\sum_{n=1}^{N}\left[\Phi_3 - (2-\nu) k_n \Phi_1\right]\left(\sin k_n y\right),$$

where k_n, Φ_0, Φ_1, Φ_2, *and* Φ_3 is indicated below:

$$k_n = \frac{n\pi}{b}, \tag{2.44}$$

$$\begin{aligned}
\Phi_0 &= A_1 e^{k_1 x} + A_2 e^{k_2 x} + A_3 e^{k_3 x} + A_4 e^{k_4 x}, \\
\Phi_1 &= A_1 k_1 e^{k_1 x} + A_2 k_2 e^{k_2 x} + A_3 k_3 e^{k_3 x} + A_4 k_4 e^{k_4 x}, \\
\Phi_2 &= A_1 k_1^2 e^{k_1 x} + A_2 k_2^2 e^{k_2 x} + A_3 k_3^2 e^{k_3 x} + A_4 k_4^2 e^{k_4 x}
\end{aligned}$$

and (2.45)

$$\Phi_0 = A_1 k_1^3 e^{k_1 x} + A_2 k_2^3 e^{k_2 x} + A_3 k_3^3 e^{k_3 x} + A_4 k_4^3 e^{k_4 x}.$$

Nodal forces also need to be considered according to the element segmentation concept. It will be obtained from equation (2.43) as

$$M_1 = M_x(0,y) = -D\sum_{n=1}^{N}\left[\Phi_2(0) - \nu k_n{}^2\Phi_0(0)\right](\sin k_n y),$$

$$V_1 = V_x(0,y) = -D\sum_{n=1}^{N}\left[\Phi_3(0) - (2-\nu)k_n\Phi_1(0)\right](\sin k_n y),$$

$$M_2 = -M_x(a,y) = D\sum_{n=1}^{N}\left[\Phi_2(a) - \nu k_n{}^2\Phi_0(a)\right](\sin k_n y)$$

and (2.46)

$$V_2 = V_x(a,y) = D\sum_{n=1}^{N}\left[\Phi_3(a) - (2-\nu)k_n\Phi_1(a)\right](\sin k_n y).$$

Matrix form of equation (2.46) is shown as

$$\begin{bmatrix} V_1 \\ M_1 \\ V_2 \\ M_2 \end{bmatrix} = D\begin{bmatrix} -[\Phi_3(0)] + (2-\nu)k_n{}^2[\Phi_1(0)] \\ -[\Phi_2(0)] + \nu k_n{}^2[\Phi_0(0)] \\ [\Phi_3(a)] - (2-\nu)k_n{}^2[\Phi_1(a)] \\ [\Phi_2(a)] - \nu k_n{}^2[\Phi_0(a)] \end{bmatrix}\begin{bmatrix} A_1 \\ A_2 \\ A_3 \\ A_4 \end{bmatrix}\sin k_n y \qquad (2.47)$$

$$\approx [F] = [G(\omega)][A],$$

where

$$[\Phi_3(x)] = [k_1{}^3 e^{k_1 x} \quad k_2{}^3 e^{k_2 x} \quad k_3{}^3 e^{k_3 x} \quad k_4{}^3 e^{k_4 x}],$$
$$[\Phi_2(x)] = [k_1{}^2 e^{k_1 x} \quad k_2{}^2 e^{k_2 x} \quad k_3{}^2 e^{k_3 x} \quad k_4{}^2 e^{k_4 x}],$$
$$[\Phi_1(x)] = [k_1 e^{k_1 x} \quad k_2 e^{k_2 x} \quad k_3 e^{k_3 x} \quad k_4 e^{k_4 x}]$$

and (2.48)

$$[\Phi_0(x)] = [e^{k_1 x} \quad e^{k_2 x} \quad e^{k_3 x} \quad e^{k_4 x}].$$

Now, all the components for the spectral element matrix are derived. Using nodal force – amplitude matrix (equation (2.47)) and nodal displacement – amplitude matrix (equation (2.39)), the spectral element matrix is obtained as

$$\begin{aligned}[F] &= [G(\omega)][A] = [G(\omega)][H(\omega)]^{-1}[d] \\ &= [S(\omega)]_e[d],\end{aligned} \tag{2.49}$$

where $[S(\omega)]_e$ is the spectral element matrix for one element in local coordinates system. For structures which have elements more than one, the spectral element matrix for one element should be combined to form a global spectral element matrix. And depends on the number of element, size of global spectral element matrix is determined. If external forces are given, nodal displacements as solutions will be obtained from

$$[F]_g = [S(\omega)]_g[d]_g \quad \Rightarrow \quad [d]_g = [S(\omega)]_g^{-1}[F]_g, \tag{2.50}$$

where $[S(\omega)]_g$, $[d]_g$, and $[F]_g$ is global spectral element matrix, global nodal displacement, and global nodal force, respectively.

The nodal displacements obtained above are used for frequency response function as

$$FRF(s,\omega) = \log_{10}\left(\frac{d(s,\omega)}{F(\omega)}\right). \tag{2.51}$$

And dynamic response also can be calculated through the inverse Fourier transform (IFT) as

$$d(\omega) \overset{IFT}{\rightarrow} d(t) = \frac{1}{2\pi}\int_{-\infty}^{\infty} d(\omega)e^{-i\omega t}d\omega. \tag{2.52}$$

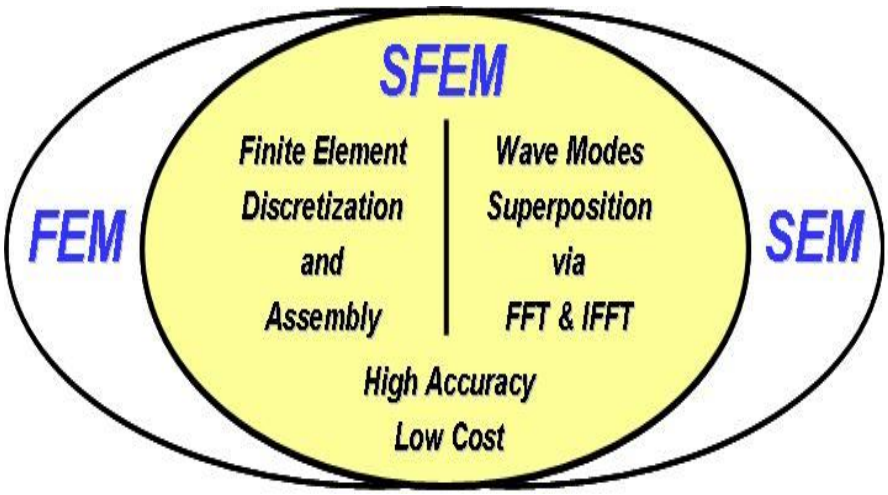

Fig. 2.1 Basic features of the Spectral Finite Element Method

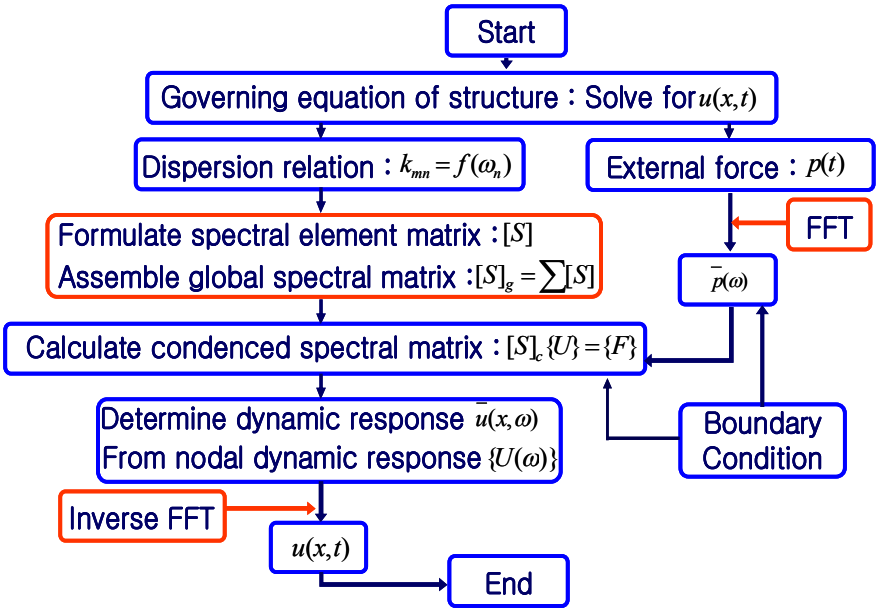

Fig. 2.2 SFEM procedure

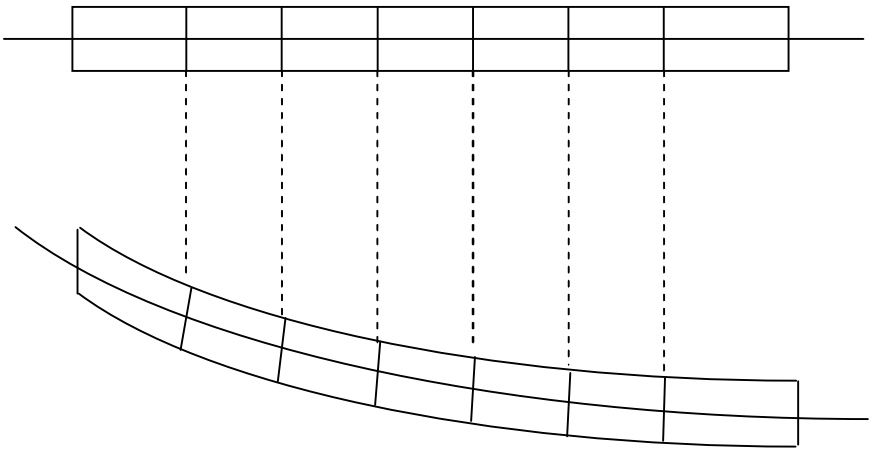

Fig. 2.3 Characteristics of the Euler beam in movement
(in an exaggerated manner)

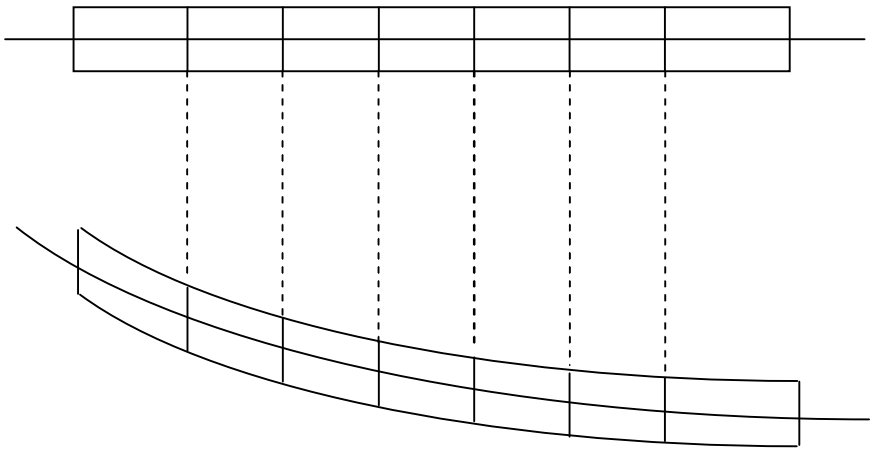

Fig. 2.4 Characteristics of the Timoshenko beam in movement
(in an exaggerated manner)

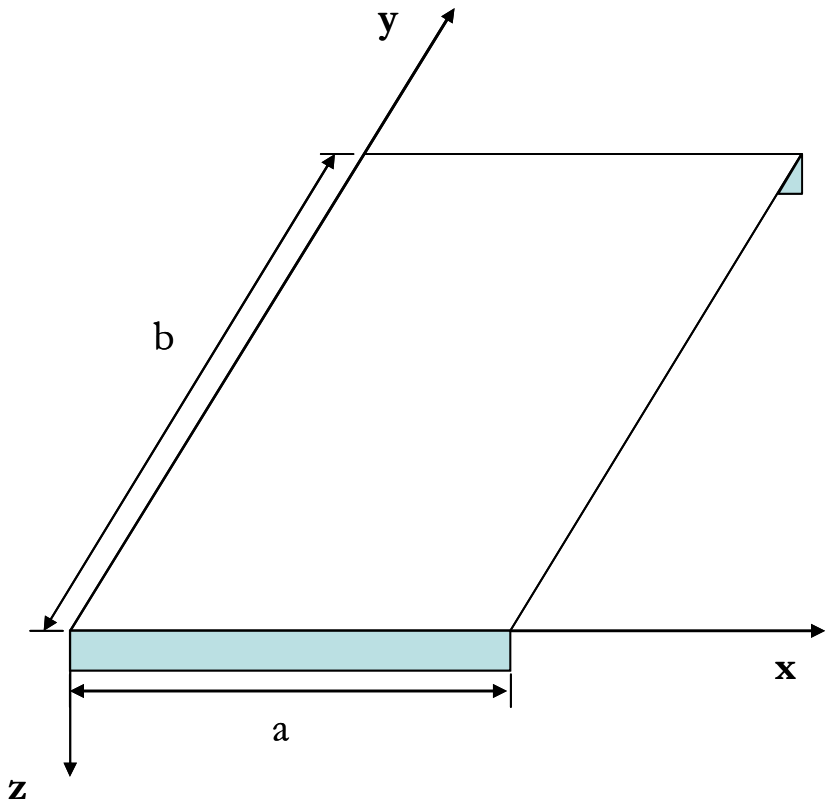

Fig. 2.5 Kirchhoff plate model

Table. 2-1 Comparison of the SFEM and the FEM

Method	Shape function	Element Segmentation	Analysis frequency	Operation time
FEM	Frequency independent static shape fucntion	Depends on analysis frequency	Error included in high-frequency range	Long operation time and a lot of memory consumption
SFEM	Frequency dependent dynamic shape function	Depends on impedance	Accurate results in all frequency range	Short operation time

3. Boundary Element Method

3.1. Introduction

The boundary element method is a numerical computational method of solving linear partial differential equations which have been formulated as integral equations. It can be applied in many areas of engineering and science including fluid mechanics, acoustics, electromagnetics, and fracture mechanics.

The integral equation may be regarded as an exact solution of the governing partial differential equation. The boundary element method attempts to use the given boundary conditions to fit boundary value into the integral equation, rather than values throughout the space defined by a partial differential equation. Once this is done, in the post-processing stage, the integral equation can then be used again to calculate numerically the solution directly at any desired point in the interior of the solution domain. The boundary element method is often more efficient than other methods, including finite elements, in terms of computational resources for problems where there is a small surface/volume ratio. Conceptually, it works by constructing a "mesh" over the modeled surface. However, for many problems boundary element methods are significantly less efficient than volume-discretization methods (finite element method, finite difference method).

Boundary element formulations typically give rise to fully populated matrices. This means that the storage requirements and computational time will tend to grow according to the square of the problem size. By contrast, finite element matrices are typically banded (elements are only locally connected) and the storage requirements for the system matrices typically grow quite linearly with the problem size. Compression techniques (e.g. multiple expansions or adaptive cross approximation/hierarchical matrices) can be used to improve these problems, though at the cost of added complexity and with a success-rate that depends heavily on the nature of the problem being solved and the geometry involved.

BEM is applicable to problems for which Green's functions can be calculated. These usually involve fields in linear homogeneous media. This places considerable restrictions on the range and generality of problems to which boundary elements can usually be applied. Nonlinearities can be included in the formulation, although they will generally introduce volume integrals which then require the volume to be discretized before solution can be attempted, removing one of the most often cited advantages of BEM. A useful technique for treating the volume integral without discretizing the volume is the dual-reciprocity method. The technique approximates part of the integrand using radial basis functions (local interpolating functions) and converts the volume integral into boundary integral after collocating at selected points distributed throughout the

volume domain (including the boundary). In the dual-reciprocity BEM, although there is no needs to discretize the volume into meshes, unknowns at chosen points inside the solution domain are involved in the linear algebraic equations approximating the problem being considered.

The Green's function elements connecting pairs of source and field patches defined by the mesh form a matrix, which is solved numerically. Unless the Green's function is well behaved, at least for pairs of patches near each other, the Green's function must be integrated over either or both the source patch and the field patch. The form of the method in which the integrals over the source and field patches are the same is called "Galerkin's method". Galerkin's method is the obvious approach for problems which are symmetrical with respect to exchanging the source and field points. In frequency domain electromagnetic this is assured by electromagnetic reciprocity.

In the process of BEM, analytical approach to integration of surface is almost impossible for many cases. Since surface for integration can be arbitrary shape, numerical integration is the only way when surface of problem is very complex. For the numerical integration, Gauss quadrature is a well known approximated method that use weighted factor to selected point for integration. In this way, integration goes simple form of summation that can be easily calculated. And the Green's functions, or fundamental solutions, are often problematic to integrate as

they are based on a solution of the system equations subject to a singularity load. Integrating such singular fields is not easy. For simple element geometries (e.g. planar triangles) analytical integration can be used. For more general elements, it is possible to design purely numerical schemes that adapt to the singularity, but at great computational cost. Of course, when source point and target element (where the integration is done) are far-apart, the local gradient surrounding the point need not be quantified exactly and becomes possible to integrate easily due to the smooth decay of the fundamental solution. But in the situation of singularity needs to be considered, use of Cauchy principle value is one of the easiest and clear way of treatment.

3.1.1. Helmholtz Equation

Wave propagates in three dimensional space with very small amplitude satisfies the linearized wave equation indicated below:

$$\nabla^2 \phi(r,t) = \frac{1}{c^2} \frac{\partial^2}{\partial t^2} \phi(r,t), \tag{3.1}$$

where k is wavenumber and defined as ω / c. e^{-jwt} term is employed with assumption of time harmonic function.

Even though many researches have been done to solve the well known wave equation (3.1) geometrically or analytically, numerical approach is only available due to the problem of variable separation. Using Green's function is one of the famous procedures for numerical approach; it helps to solve the problem with proper distribution of monopole and dipole source. And it is important to think boundary conditions which are applied to the Helmholtz equation (equation (3.1)) differently with physical property of surface. When boundary is presented as rigid or vibrating surface, boundary condition is shown as

$$\frac{\partial \phi}{\partial n} = f(r) . \tag{3.2}$$

Rigid boundary condition means velocity is zero at the surface, in other words $f(r)$ in equation (3.2) is zero ($f(r)$=0). And $f(r)$ goes to $-iw\rho v_n(r)$ for vibrating boundary condition ($f(r) = -i\omega\rho v_n(r)$). Here, v_n means vibrating velocity of surface. In the case of free boundary, boundary condition can be shown as

$$\phi(r) = 0 . \tag{3.3}$$

All waves that includes radiated noise, scattered wave, and waves from boundary conditions (equation (3.2) and (3.3)) should satisfy the Sommerfeld radiation condition. This condition means that all waves go outward in infinite medium and is presented as

$$\lim_{r\to\infty}\left[r\left\{ \frac{\partial\phi(r)}{\partial r} + ik\phi(r) \right\} \right] = 0 . \tag{3.4}$$

3.1.2. Integration Equation of Direct BEM

Helmholtz equation is derived from the wave equation with Green's theorem and function which governs the sound field. In the assumption of time harmonic wave in free space, Green's function satisfies the Helmholtz equation with point source:

$$\nabla^2 G(r,r') + k^2 G(r,r') = -4\pi\delta(r-r') , \tag{3.5}$$

where $G(r,r')$ is Green's function, $\delta(r-r')$ is Dirac delta function, 4π means unit flux at r' from center of small sphere. And minus sign indicates external flux from source.

Solution for equation (3.5) is

$$G(r,r') = -\frac{i}{4}H_0^{(2)}(kR) \qquad \text{for 2-D}$$

and (3.6)

$$G(r,r') = \frac{1}{4\pi}\frac{e^{-ikR}}{R} \qquad \text{for 3-D,}$$

where $R = |r - r'|$, $H_0^{(2)}$ is a zero order 2nd kind Hankel function.

Equation (3.6) is Green's function for two dimensional spaces and three dimensional spaces, respectively. And these two equations satisfy the Sommerfeld radiation condition in infinite space (equation (3.4)). Using Green's 2nd theorem that relates integration for volume and surface, the equation can be shown with analytic and continuous function ϕ and ψ as

$$\int_V [\phi(\nabla^2 + k^2)\psi - \psi(\nabla^2 + k^2)\phi]dV = \int_S \left[\phi\frac{\partial\psi}{\partial n} - \psi\frac{\partial\phi}{\partial n}\right]dS, \qquad (3.7)$$

where surface vector is obtained from product of surface area (dS) and normal unit vector to the surface.

Advanced form of equation (3.7) is given by substituting equation (3.5) and

(3.6) into equation (3.7) as

$$-\int_V \left[p\nabla^2\left(\frac{e^{-ikR}}{4\pi R}\right) - \frac{e^{-ikR}}{4\pi R}\nabla^2 p \right] dV = \int_{S_0} \left[\frac{e^{-ikR}}{4\pi R}\frac{\partial p}{\partial n} - p\frac{\partial}{\partial n}\left(\frac{e^{-ikR}}{4\pi R}\right) \right] dS + I_\infty , \tag{3.8}$$

where p is pressure and I_∞ is surface integration on the surface area when R is infinity (S_∞). Based on the Sommerfeld radiation condition, integration value at infinity (I_∞) is zero. So, the Kirchhoff-Helmholtz equation is obtained as

$$c(r)p(r) = \int_{S_0} \left[p(r_0)\frac{\partial}{\partial n}\left(\frac{e^{-ikR}}{R}\right) - \frac{\partial p(r_0)}{\partial n}\frac{e^{-ikR}}{R} \right] dS , \tag{3.9}$$

where $\frac{\partial}{\partial \mathrm{n}}$ means surface normal derivative, r_0 is a point on surface S_0 as indicated in Fig. 3.1. And the value of $c(r)$ in equation (3.9) is determined by geometrical characteristics of surface at r position as

$$c(r)=\begin{cases}4\pi & for \quad r\in V \quad and \quad r\notin S_0 \\ 4\pi-\int_{S_0}\frac{\partial}{\partial n}\left[\frac{1}{R(r,r_0)}\right]dS(r_0) & \\ & for \quad r\notin V \quad and \quad r\notin S_0 \\ 0 & for \quad r\in V \quad and \quad r\in S_0\end{cases} . \qquad (3.10)$$

Second one in equation (3.10) can show singularity in the integration process when field point indicates same position with boundary point. This problem can be solved with introduction of the Cauchy principle value. If boundary surface is smooth, the value shows 2π which means solid angle.

First and second term on the right hand side in equation (3.8) represents physical influence of dipole on r_0 that points out $\cos\theta$ to normal direction of surface with amplitude $p(r_0)$ and of monopole on r_0 that has amplitude $i\omega\rho v_n(r_0)$ at $p(r)$. Therefore, mathematical model for the pressure can be formulated with distribution of dipole and monopole whatever the boundary surface shape is. In other words, it is possible to get the pressures at any points using the information of pressure and particle velocity at the boundary surface.

3.1.3. Segmentation of Integral Equation

Equation (3.9) is a similar form of 2nd kind Fredholm integral equation as

indicated below:

$$-\lambda\phi(p)+\int_S x(p,q)f(q)\,dS=f(p) \qquad for\ p\in S\,. \tag{3.11}$$

Collocation method is famous one to solve this kind of integral equation.

3.1.4. Geometrical Discretization of Surface

$\widetilde{S}$ is a approximated boundary surface of S with panels ΔS_j (j =1, 2, 3, ⋯, N) that satisfy this equation $\widetilde{S}=\sum_{j=1}^{N}\Delta S_j$. Fig. 3.2 shows approximated boundary surface $\widetilde{S}$ that consists of N panels. This boundary surface approximation is for discretization of the terms in the Helmholtz equation which is derived previously. And integration at panels can be generalized because all the panels are in similar shape. This will help to construct the boundary surface with data structure. To express boundary surface in the form of data structure, mesh points and grid are required to separate panels and represents coordinate value.

Prediction of sound pressure using the boundary element method brings numerical error caused by the boundary surface discretization. This numerical error can be reduced when boundary surface modeling is properly done. To make

the given boundary surface well discretized, interpolation function needs to be considered on pressure, normal velocity, and coordinates in the basis of collocation points as indicated below:

$$x_i(\xi) = \sum_j N_j(\xi) x_{ij} \ , \tag{3.12}$$

$$p_i(\xi) = \sum_j N_j(\xi) p_{ij} \tag{3.13}$$

and

$$v_i(\xi) = \sum_j N_j(\xi) v_{ij} \ , \tag{3.14}$$

where j means mesh points and $N_j(\xi)$ is shape function in local coordinates $\xi = (\xi_1, \xi_2)$. But in this paper, shape function is not used because the entire boundary surface is modeled using constant element. And enough mesh points are used for surface discretization to make the numerical error small in the process.

3.1.5. Boundary Value Calculation with Boundary Conditions

The direct boundary element method requires pressure and particle velocity at the surface to solve the Helmholtz integral equation. So, it is essential to calculate

another boundary value from one given boundary condition. For the first step, we locate field points at the boundary points and discretize the integral equation by substituting equation (3.12), (3.13), and (3.14) into (3.9). Then, equation (3.9) becomes

$$\sum_{m=1}^{N}\sum_{j} a^{j}{}_{mk}\, p_{mj} - \left(4\pi + \sum_{m=1}^{N} C_{mk}\right) p_k = \sum_{m=1}^{N}\sum_{j} b^{j}{}_{mk}\, v_{mj} \quad , \quad \text{for } k = 1, 2, \cdots, L \tag{3.15}$$

where p_j means pressure at mesh point j, L is total number of mesh points, and N is total number of discretized elements. $a^{j}{}_{mk}$, $b^{j}{}_{mk}$ and C_{mk} is defined as

$$a^{j}{}_{mk} = \int_{S_m} N_j(\xi) \frac{\partial}{\partial n}\left(\frac{e^{-ikR_{mk}(\xi)}}{R_{mk}(\xi)}\right) J(\xi)\, d\xi \,, \tag{3.16}$$

$$b^{j}{}_{mk} = i\omega\rho \int_{S_m} N_j(\xi)\left(\frac{e^{-ikR_{mk}(\xi)}}{R_{mk}(\xi)}\right) J(\xi) d\xi \tag{3.17}$$

and

$$C_{mk} = \int_{S_m} \frac{\partial}{\partial n}\left(\frac{1}{R_{mk}(\xi)}\right) J(\xi) d\xi \,, \tag{3.18}$$

where $J(\xi)$ is Jacobian, S_m indicates area of mth element, and $R_{mk}(\xi)$ is a length between mesh points k and element m.

Equation (3.15), (3.16), (3.17), and (3.18) shows equation can be rearranged with L linear algebra equations that have pressure p and velocity v at the surface. Simple form of the equation is

$$[A]\{p\}_s = [B]\{v\}_s, \tag{3.19}$$

where $\{p\}_s$ is pressure and $\{v\}_s$ is velocity at the boundary surface that is given or calculated from boundary conditions. If surface boundary velocity is given, equation (3.19) can be solved with inverse of matrix A (Neumann boundary condition):

$$\{p\}_s = [A]^{-1}[B]\{v\}_s. \tag{3.20}$$

Or, if surface pressure is given, equation (3.19) can be solved with inverse of matrix B (Dirichlet boundary condition):

$$\{v\}_s = [B]^{-1}[A]\{p\}_s. \tag{3.21}$$

In this paper, boundary displacements are given for boundary conditions. So, appropriate treatment will be given in detail later.

3.1.6. Pressure or Velocity Calculation with Boundary Conditions

By using two boundary conditions calculated in section 3.1.5, it is possible to get the pressure and surface velocity at any points. And to make numerical approach available, discretization of equation (3.9) and (3.10) is necessary.

For particle velocity at field point, the Euler equation is used:

$$\rho \frac{\partial v}{\partial t} = -\nabla p \,. \tag{3.22}$$

After substituting equation (3.9) into the Euler equation (equation (3.22)), particle velocity at field point can be calculated with derivative of pressure in each direction. That is

$$v_x = -\frac{1}{4\pi i \omega \rho} \int_{S_0} p(r_0) F_x dS - \frac{1}{4\pi} \int_{S_0} v_n G_x dS \,, \tag{3.23}$$

$$v_y = -\frac{1}{4\pi i \omega \rho} \int_{S_0} p(r_0) F_y dS - \frac{1}{4\pi} \int_{S_0} v_n G_y dS \tag{3.24}$$

and

$$v_z = -\frac{1}{4\pi i\omega\rho}\int_{S_0} p(r_0)F_z dS - \frac{1}{4\pi}\int_{S_0} v_n G_z dS, \tag{3.25}$$

where v_x, v_y, and v_z represents boundary velocity in x-, y-, and z- direction, respectively. F_x, G_x, F_y, G_y, F_z, and G_z is defined as

$$G_x = -(ikR+1)\frac{e^{-ikR}}{R^2}\frac{(x-x_0)}{R}, \tag{3.26}$$

$$\begin{aligned} F_x = {} & (2+2ikR-k^2R^2)\frac{e^{-ikR}}{R^3}\frac{(x-x_0)}{R}\frac{\vec{R}\cdot\vec{n}}{R} \\ & -(ikR+1)\left\{\left(\frac{1}{R}-\frac{(x-x_0)^2}{R^3}\right)n_1 - \frac{(x-x_0)(y-y_0)}{R^3}n_2\right. \\ & \left. -\frac{(x-x_0)(z-z_0)}{R^3}n_3\right\}\frac{e^{-ikR}}{R^2}, \end{aligned} \tag{3.27}$$

$$\begin{aligned} F_y = {} & (2+2ikR-k^2R^2)\frac{e^{-ikR}}{R^3}\frac{(y-y_0)}{R}\frac{\vec{R}\cdot\vec{n}}{R} \\ & -(ikR+1)\left\{-\frac{(x-x_0)(y-y_0)}{R^3}n_1 + \left(\frac{1}{R}-\frac{(y-y_0)^2}{R^3}\right)n_2\right. \\ & \left. -\frac{(y-y_0)(z-z_0)}{R^3}n_3\right\}\frac{e^{-ikR}}{R^2}, \end{aligned} \tag{3.28}$$

$$G_y = -(ikR+1)\frac{e^{-ikR}}{R^2}\frac{(y-y_0)}{R}, \tag{3.29}$$

$$F_z = (2 + 2ikR - k^2R^2)\frac{e^{-ikR}}{R^3}\frac{(z-z_0)}{R}\frac{\vec{R}\cdot\vec{n}}{R}$$
$$-(ikR+1)\left\{-\frac{(x-x_0)(z-z_0)}{R^3}n_1 - \frac{(y-y_0)(z-z_0)}{R^3}n_2 \right. \quad (3.30)$$
$$\left. + \left(\frac{1}{R} - \frac{(z-z_0)^2}{R^3}\right)n_3\right\}\frac{e^{-ikR}}{R^2}$$

and

$$G_y = -(ikR+1)\frac{e^{-ikR}}{R^2}\frac{(z-z_0)}{R}. \quad (3.31)$$

After the discretization process on equation (3.9) and (3.23) ~ (3.31), expressions become simple as

$$4\pi p_j = \sum_{m=1}^{N}\sum_{j} a^j{}_{mk} - \sum_{m=1}^{N}\sum_{j} b^j{}_{mk} v_{mj} \quad (3.32)$$

and

$$4\pi v_j = \sum_{m=1}^{N}\sum_{j} c^j{}_{mk} - \sum_{m=1}^{N}\sum_{j} d^j{}_{mk} v_{mj}\,, \quad (3.33)$$

where $a^j{}_{mk}$, $a^j{}_{mk}$, $a^j{}_{mk}$, and $a^j{}_{mk}$ are shown as indicated below:

$$a^j{}_{mk} = \int_{S_m} N_j(\xi)\frac{\partial}{\partial n}\left(\frac{e^{-ikR_k(\xi)}}{R_k(\xi)}\right)J(\xi)d\xi\,, \quad (3.34)$$

$$b^{j}{}_{mk} = i\omega\rho \int_{S_m} N_j(\xi) \frac{\partial}{\partial n}\left(\frac{e^{-ikR_k(\xi)}}{R_k(\xi)} \right) J(\xi) d\xi \,, \tag{3.35}$$

$$c^{j}{}_{mk} = \int_{S_m} N_j(\xi) \nabla_j \left[\frac{\partial}{\partial n}\left(\frac{e^{-ikR_k(\xi)}}{R_k(\xi)} \right) \right] J(\xi) d\xi \tag{3.36}$$

and

$$d^{j}{}_{mk} = i\omega\rho \int_{S_m} N_j(\xi) \nabla_j \left[\frac{\partial}{\partial n}\left(\frac{e^{-ikR_k(\xi)}}{R_k(\xi)} \right) \right] J(\xi) d\xi \,. \tag{3.37}$$

For numerical operation, it is convenient to express the Equation (3.32) and (3.33) in matrix form:

$$\{p\}_f = [M]_f \{v\}_s + [D]_f \{p\}_s \,. \tag{3.38}$$

3.2. Advantages and Disadvantages of BEM

This section deals with a systematic enumeration of the advantages and disadvantages of the BEM as compared with the FEM, which is presently considered the most popular and widely used numerical method in engineering mechanics.

3.2.1. Advantages of BEM

The BEM presents some distinct advantages, such as

(1) It is a general numerical method with a wide range of applications in engineering mechanics. It enjoys a firm mathematical basis and constitutes a practical and efficient computational tool. It is applicable to both linear and nonlinear problems, provided that the latter ones are or can be approximated as incrementally linear.

(2) It usually requires only a surface discretization and not a discretization of both the interior and the surface of the domain of interest as in 'domain' type techniques like the FEM. This reduction of the spatial dimensions of the problem by one greatly facilitates the data preparation

job, permits an easy conduction of mesh refinement studies and leads to a system of algebraic equations much smaller than the one encountered in the FEM.

(3) The facts that the approximations involved in the method are confined to the surface of the domain and that the influence matrices associated with the BEM consist of dominant elements on or near their main diagonal due to the singular nature of the employed Green's functions are the reasons for obtaining results of higher accuracy than by the FEM, especially in problems involving sharp gradients of the unknown functions. This accuracy of the method can be considerably increased by employing sophisticated elements and highly accurate numerical integration techniques.

(4) The employment of the Green's function or fundamental singular solution associated with the problem of interest makes possible the easy treatment of infinite or semi-infinite domains without artificial "box-type" discretization as it is the case with the FEM

(5) The above advantages of the BEM over the FEM are greatly pronounced in linear problems characterized by three-dimensional (especially infinite or semi-infinite), homogeneous and isotropic domains.

(6) The method is capable of providing values of the unknowns in the interior of the domain in a pointwise fashion so that no inter-element continuity problems can arise as in the FEM. In addition the computation is restricted to points of interest and does not involve all the mesh points as in the FEM.

(7) The BEM can be used for the construction of stiffness matrices for homogeneous very big finite elements (super-elements) or infinite elements which can be used in a finite element formulation characterized by a drastic reduction in the number of unknowns of the system.

3.2.2. Disadvantages of BEM

As any other approximate method, the BEM is also characterized by a number of disadvantages, such as

(1) It is associated with non-symmetric and fully populated influence matrices in contrast to the FEM, which involves symmetric and sparse matrices that require less computational effort for their inversion. The order of the former matrices is, however, much lower than that of the latter and their numerical treatment can be done efficiently through

special schemes. Besides, the former matrices are numerically well conditioned.

(2) It is very difficult or practically impossible to obtain the fundamental solutions for some types of problems, especially for those involving strong anisotropies and inhomogeneities, while sometimes the expressions for these solutions are too complicated or known in discrete form leading to inefficient schemes. Of course, approximate fundamental solutions in conjunction with an iterative approach can be employed at an increased computational cost. The FEM is a better choice for problems characterized by rapidly changing physical properties in the domain.

(3) The BEM is inefficient as compared with the FEM for problems with geometry for their mathematical model characterized by one or two spatial dimensions disproportionally small with respect to the others but dimensionally effective, such as those involving the analysis of moderately thick plates and shells or thin narrow strips. The BEM is also inefficient for one-dimensional problems, such as those involving the analysis of beams and frameworks.

(4) The presence of known distributed body forces in linear problems or pseudo-incremental body forces in nonlinear problems creates volume integrals which require an internal discretization of the domain. However, this internal discretization is much simpler than that of the FEM, can be restricted to a small portion of the domain in some cases and most importantly, does not lead in any increase in the order of the final system of algebraic equations.

(5) There are very few special and general-purpose BEM computer programs presently available as compared with the great number of corresponding FEM programs. This is because the BEM is still in the stage of development, competes against a very efficient and well established technique, the FEM and the architecture of a BEM computer program is not conceptually as easy as the one for the FEM.

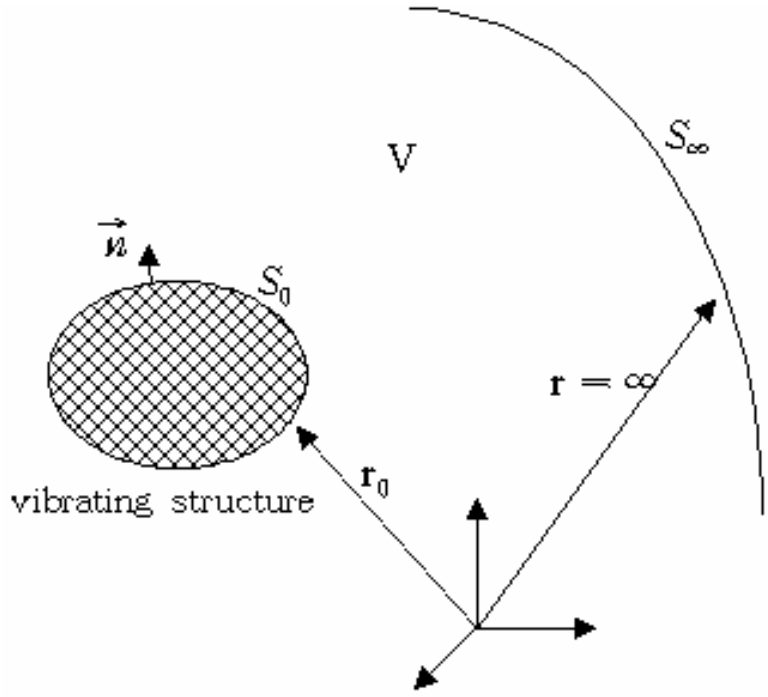

Fig. 3.1 Illustration of geometrical conditions

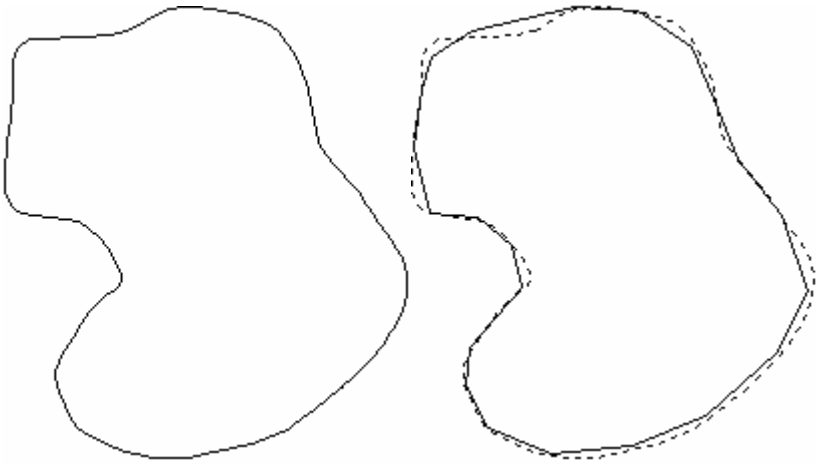

(a) Original boundary surface (b) Discretized boundary surface

Fig. 3.2 Boundary surface discretization

4. Structural Vibration Analysis of Circular Cylindrical Shell

4.1. Governing Equation of Circular Cylindrical Shell

Classical theory of thin shell with small displacement is based on the following assumptions made by Love.

(1) The thickness of the shell is small compared with the other dimensions, for example, the smallest radius of curvature of the middle surface of the shell.

(2) Strains and displacements are sufficiently small so that the quantities of second- and higher-order magnitude in the strain-displacement relations may be neglected in comparison with the first-order terms.

(3) The transverse normal stress is small compared with the other normal stress components and maybe neglected.

(4) Normals to the undeformed middle surface remain straight and normal to the deformed middle surface and suffer no extension.

These assumptions are generally accepted in the derivation of thin shell theory.

For the analysis on circular cylindrical shell, cylindrical coordinates are generally used. But in this paper, shell based coordinates are introduced to express the strains and stresses in efficient way. (See Fig. 4.1 and Fig. 4.2)

To derive the governing equation of circular cylindrical shell, Hamilton's principal is used. But before we apply Hamilton's principle, strains of circular cylindrical shell should be considered since strain and kinetic energy are expressed with the strains. So in this section, deformation of curved beam is considered first and then expands this deformation from two to three dimensional spaces for the strains of circular cylindrical shell.

4.1.1. Deformation of Curved Beams

In the cylindrical coordinate system, (r, Θ, z), the components of the displacement vector in the plane are denoted by $\bar{u}_r$ and $\bar{u}_\theta$. The strains are related to these displacements by

$$\bar{\varepsilon}_{rr} = \frac{\partial \bar{u}_r}{\partial r}, \tag{4.1}$$

$$\bar{\varepsilon}_{\theta\theta} = \frac{\bar{u}_r}{r} + \frac{1}{r}\frac{\partial \bar{u}_\theta}{\partial \theta} \tag{4.2}$$

and

$$\bar{\varepsilon}_{r\theta} = \frac{1}{2}\left(\frac{1}{r}\frac{\partial \bar{u}_r}{\partial \theta} + \frac{\partial \bar{u}_\theta}{\partial r} - \frac{\bar{u}_\theta}{r} \right). \tag{4.3}$$

And based on the assumption of small thickness in r direction, expand the displacements in a Taylor series about the mid-plane (r=R) using the variable $\xi = r - R$. That is,

$$\bar{u}_r(r,\theta) \approx u_r(\theta) \tag{4.4}$$

and

$$\bar{u}_\theta(r,\theta) \approx u_\theta(\theta) - \xi\psi_\theta(\theta), \tag{4.5}$$

where ψ_θ is a rotation of the subscripted face in the direction of the curvature.

Since approximated displacements are functions of θ not r, derivative with respect to r can be replaced with R. And using equation (4.4) and (4.5), shear strain is

$$\bar{\varepsilon}_{r\theta} = \frac{1}{2}\left(\frac{1}{R}\frac{\partial u_r}{\partial \theta} - \psi_\theta - \frac{u_\theta}{R} + \frac{\xi}{R}\psi_\theta \right). \tag{4.6}$$

The transverse shear strains are negligible on average because the beam is slender. This leads to

$$\psi_\theta \approx \frac{1}{R}\frac{\partial u_r}{\partial \theta} - \frac{u_\theta}{R}. \tag{4.7}$$

Assume that ξ / R is small compared to unity. The approximate deformation relations, equation (4.4) and (4.5), are now

$$\overline{u}_r(r,\theta) \approx u_r(\theta) \tag{4.8}$$

and

$$\overline{u}_\theta(r,\theta) \approx u_\theta(\theta) - \xi\left(\frac{1}{R}\frac{\partial u_r}{\partial \theta} - \frac{u_\theta}{R}\right). \tag{4.9}$$

These give the only nonzero strain component as

$$\varepsilon_{\theta\theta} = \frac{u_r}{R} + \frac{1}{R}\frac{\partial u_\theta}{\partial \theta} - \frac{\xi}{R^2}\left(\frac{\partial^2 u_r}{\partial \theta^2} - \frac{\partial u_\theta}{\partial \theta}\right). \tag{4.10}$$

To convert this strain component from cylindrical based coordinates to shell based coordinates, use

$$R\theta \rightarrow s, \qquad r \rightarrow -y. \tag{4.11}$$

Then, corresponding displacement is

$$u_\theta \rightarrow u, \qquad u_r \rightarrow -v. \tag{4.12}$$

And approximate deformation relations become

$$\bar{u}(s,y) \approx u(s) - y\left(\frac{\partial v}{\partial s} + \frac{u}{R}\right) \quad and \quad \bar{v}(s,y) \approx v(s). \tag{4.13}$$

Using equation (4.2), (4.12) and (4.13), nonzero strain can be expressed as

$$\varepsilon_{ss} = \frac{\partial u}{\partial s} - \frac{v}{R} - y\left(\frac{\partial^2 v}{\partial s^2} + \frac{1}{R}\frac{\partial u}{\partial s}\right). \tag{4.14}$$

4.1.2. Deformation of Cylindrical Shells

In this section, deformation of cylindrical shell is considered to get strains. Strain obtaining procedure for cylindrical shell is similar with the one for curved beams but variation of response with respect to the lengthwise z direction is included.

Following the procedure established in previous section, approximated defor-

mations of the shell in cylindrical coordinates are

$$\overline{u}_r(r,\theta,z) \approx u_r(\theta,z), \tag{4.15}$$

$$\overline{u}_\theta(r,\theta,z) \approx u_\theta(\theta,z) - \xi\left(\frac{1}{R}\frac{\partial u_r}{\partial \theta} - \frac{u_\theta}{R}\right) \tag{4.16}$$

and

$$\overline{u}_z(r,\theta,z) \approx u_z(\theta,z) - \xi\frac{\partial u_r}{\partial z}, \tag{4.17}$$

where $\xi \equiv (r-R)$ and equation (4.17) allow bending terms in the z axis. Strains in cylindrical coordinates can be simply obtained from rectangular coordinates by transforming. Those are

$$\varepsilon_{zx} = \left(\varepsilon_{zr}\cos\theta - \varepsilon_{z\theta}\sin\theta\right) \tag{4.18}$$

and

$$\begin{aligned} 2\varepsilon_{zx} &= \left(\frac{\partial u_z}{\partial x} + \frac{\partial u_x}{\partial z}\right) \\ &= \left(\cos\theta\frac{\partial}{\partial r} - \frac{\sin\theta}{r}\frac{\partial}{\partial\theta}\right)u_z + \frac{\partial}{\partial z}\left(u_r\cos\theta - u_\theta\sin\theta\right) \\ &= \left(\frac{\partial u_z}{\partial r} - \xi\frac{\partial^2 u_r}{\partial r\partial z} + \frac{\partial u_r}{\partial z}\right)\cos\theta \\ &\quad -\left(\frac{1}{r}\frac{\partial u_z}{\partial\theta} + \frac{\partial u_\theta}{\partial z} - \frac{\xi}{r}\left(2\frac{\partial^2 u_r}{\partial\theta\partial z} - \frac{\partial u_\theta}{\partial z}\right)\right)\sin\theta. \end{aligned} \tag{4.19}$$

Then, arrange the equation (4.18) and (4.19) for cylindrical coordinates as

$$2\varepsilon_{zr} = \left(\frac{\partial u_z}{\partial r} - \xi \frac{\partial^2 u_r}{\partial r \partial z} + \frac{\partial u_r}{\partial z} \right) \tag{4.20}$$

and

$$2\varepsilon_{z\theta} = \frac{1}{r}\frac{\partial u_z}{\partial \theta} + \frac{\partial u_\theta}{\partial z} - \frac{\xi}{r}\left(2\frac{\partial^2 u_r}{\partial \theta \partial z} - \frac{\partial u_\theta}{\partial z} \right). \tag{4.21}$$

Since deformation is approximated with variable Θ and z based on assumption of small dimension in r direction, nonzero strains are also expressed with those two variables as

$$\bar{\varepsilon}_{zz} = \frac{\partial u_z}{\partial z} - \xi \frac{\partial^2 u_r}{\partial z^2} \tag{4.22}$$

and

$$2\bar{\varepsilon}_{\theta z} = \frac{1}{R}\frac{\partial u_z}{\partial \theta} + \frac{\partial u_\theta}{\partial z} - \frac{\xi}{R}\left(2\frac{\partial^2 u_r}{\partial z \partial \theta} - \frac{\partial u_\theta}{\partial z} \right). \tag{4.23}$$

$\varepsilon_{\theta\theta}$ is already shown in equation (4.10).

It is worth while to convert strains above to shell based form. For shell based

coordinates, it is typical to have a hoop coordinate s, an axial coordinate y, and a transverse coordinate z pointed toward the origin of the circle:

$$R\theta \to s, \qquad z \to -y, \qquad r \to -z\,. \tag{4.24}$$

This gives the corresponding displacements as

$$u_\theta \to u, \qquad u_z \to -v, \qquad u_r \to -w \tag{4.25}$$

Then, reconstruct approximate deformation relations using equation (4.15), (4.16), (4.17) and (4.25) as

$$\overline{u}(s,y,z) \approx u(s,y) - z\left(\frac{\partial w}{\partial s} + \frac{u}{R}\right), \tag{4.26}$$

$$\overline{v}(s,y,z) \approx v(s,y) - z\frac{\partial w}{\partial y} \tag{4.27}$$

and

$$\overline{w}(s,y,z) \approx w(s,y)\,. \tag{4.28}$$

Finally, nonzero strains with the notation of shell based coordinates are obtained.

$$\varepsilon_{ss} = -\frac{w}{R} + \frac{\partial u}{\partial s} - z\left(\frac{\partial^2 w}{\partial s^2} + \frac{1}{R}\frac{\partial u}{\partial s}\right), \tag{4.29}$$

$$\varepsilon_{yy} = \frac{\partial v}{\partial y} - z\frac{\partial^2 w}{\partial y^2} \tag{4.30}$$

and

$$2\varepsilon_{sy} = \frac{\partial v}{\partial s} + \frac{\partial u}{\partial y} - z\left(2\frac{\partial^2 w}{\partial s \partial y} + \frac{1}{R}\frac{\partial u}{\partial y}\right). \tag{4.31}$$

4.1.3. Hamilton's Principle

To derive equation of motion of circular cylindrical shell, it is advantageous to use Hamilton's principle because boundary conditions are also specified consistently. Hamilton's principle consists of three components. These are strain energy, kinetic energy and potential of applied loads. After getting these components, Hamilton's principle can be expressed as

$$\delta \int_{t1}^{t2} [T - (U + V)] dt = 0 . \tag{4.32}$$

The strain energy for a small segment of shell in plane stress is

$$U = \frac{1}{2}\int_{\forall}\left[\frac{E}{\left(1-\nu^2\right)}\left(\varepsilon_{ss}^2 + \varepsilon_{yy}^2 + 2\nu\varepsilon_{ss}\varepsilon_{yy}\right) + G\gamma_{sy}^2\right] d\forall . \qquad (4.33)$$

Substitute for the strains and integrate with respect to the thickness to get the total strain energy as

$$U = \frac{1}{2}\int_s\int_y \left[\overline{E}U_1 + DU_2\right] ds\, dy , \qquad (4.34)$$

where

$$U_1 = \left(\frac{\partial u}{\partial s} + \frac{\partial v}{\partial y} - \frac{w}{R}\right) + \frac{1}{2}(1-\nu)\left[-4\left(\frac{\partial u}{\partial s} - \frac{w}{R}\right)\frac{\partial v}{\partial y} + \left(\frac{\partial u}{\partial y} + \frac{\partial v}{\partial s}\right)^2\right],$$

$$U_2 = \left(\frac{\partial^2 w}{\partial s^2} + \frac{\partial^2 w}{\partial y^2} + \frac{1}{R}\frac{\partial u}{\partial s}\right)^2 - 2(1-\nu)\frac{\partial^2 w}{\partial y^2}\left(\frac{\partial^2 w}{\partial s^2} + \frac{1}{R}\frac{\partial u}{\partial s}\right)$$
$$+ \frac{1}{2}(1-\nu)\left(2\frac{\partial^2 w}{\partial s \partial y} + \frac{1}{R}\frac{\partial u}{\partial y}\right)^2 ,$$

$D \equiv Eh^3/12\left(1-\nu^2\right)$ and $\overline{E} = Eh/\left(1-\nu^2\right)$. In the above, U_1 represents the strain energy due to the membrane strains while U_2 represents the contribution from the bending strains.

The total kinetic energy is

$$T = \frac{1}{2}\int_{\forall} \rho\left[\dot{\bar{u}}(x,y,z,t)^2 + \dot{\bar{v}}(x,y,z,t)^2 + \dot{\bar{w}}(x,y,z,t)^2\right]$$
$$= \frac{1}{2}\int_s \int_y \rho h\left[\dot{u}^2 + \dot{v}^2 + \dot{w}^2\right] ds\, dy, \tag{4.35}$$

where rotational inertia term is neglected.

Let the potential of the applied loads be

$$\delta V = -Q_u u - Q_v v - Q_w w - Q_\psi \psi, \tag{4.36}$$

where, $\psi \equiv \partial w / \partial s$. And the associated boundary conditions on the side s=constant are specified in terms of one each of the following pairs:

$$Q_u = \overline{E}\left[\frac{\partial u}{\partial s} - \frac{w}{R} + \nu\frac{\partial v}{\partial y}\right] + \frac{D}{R}\left[\frac{\partial^2 w}{\partial s^2} + \frac{1}{R}\frac{\partial u}{\partial s} + \nu\frac{\partial^2 w}{\partial y^2}\right],$$
$$Q_v = \frac{1}{2}(1-\nu)\overline{E}\left[\frac{\partial v}{\partial s} + \frac{\partial u}{\partial y}\right],$$
$$Q_w = -\frac{D}{R}\left[\frac{\partial^2 u}{\partial s^2} + (1-\nu)\frac{\partial^2 u}{\partial y^2}\right] - D\left[\frac{\partial^3 w}{\partial s^3} + (2-\nu)\frac{\partial^3 w}{\partial s \partial y^2}\right]$$

and

$$Q_\psi = D\left[\frac{\partial^2 w}{\partial s^2} + \nu\frac{\partial^2 w}{\partial y^2} + \frac{1}{R}\frac{\partial u}{\partial s}\right]. \tag{4.37- 4.40}$$

Later on, these boundary conditions in the above (equation (4.37- 4.40)) relate to resultant force to construct stiffness matrix in displacement – force relation.

Based on calculated strain energy, kinetic energy, potential of applied loads (equation (4.34), (4.35) and (4.36)), equation (4.32) can be reconstructed and taking the variation with respect to $\delta u, \delta v$ and δw leads to three governing equations, which is

$$\begin{aligned}&\overline{E}\left[\frac{\partial^2 u}{\partial s^2}+\frac{1}{2}(1-\nu)\frac{\partial^2 u}{\partial y^2}+\frac{1}{2}(1+\nu)\frac{\partial^2 v}{\partial s\partial y}-\frac{1}{R}\frac{\partial w}{\partial s}\right]\\&+\frac{D}{R}\left[\frac{\partial^2 u}{\partial s^2}+\frac{1}{2}(1-\nu)\frac{\partial^2 u}{\partial y^2}+R\frac{\partial^3 w}{\partial y^2\partial s}+R\frac{\partial^3 w}{\partial s^3}\right]=\rho h\frac{\partial^2 u}{\partial t^2},\end{aligned} \tag{4.41}$$

$$\overline{E}\left[\frac{1}{2}(1+\nu)\frac{\partial^2 u}{\partial s\partial y}+\frac{\partial^2 v}{\partial y^2}+\frac{1}{2}(1-\nu)\frac{\partial^2 v}{\partial s^2}-\frac{\nu}{R}\frac{\partial w}{\partial y}\right]=\rho h\frac{\partial^2 v}{\partial t^2} \tag{4.42}$$

and

$$\begin{aligned}&-\overline{E}\left[\frac{1}{R}\frac{\partial u}{\partial s}+\frac{\nu}{R}\frac{\partial v}{\partial y}-\frac{w}{R^2}\right]\\&+D\left[\frac{\partial^4 w}{\partial s^4}+2\frac{\partial^4 w}{\partial s^2\partial y^2}+\frac{\partial^4 w}{\partial y^4}\right]+\frac{D}{R}\left[\frac{\partial^3 u}{\partial y^2\partial s}+\frac{\partial^3 u}{\partial s^3}\right]=-\rho h\frac{\partial^2 w}{\partial t^2}.\end{aligned} \tag{4.43}$$

4.2. Spectral Formulation of Circular Cylindrical Shell

Obtaining the spectral stiffness matrix for circular cylindrical shell in the displacement – force relation is a main object in this section. To set displacement and force, general solution should be defined first. Wavenumber calculation is a important part of constructing general solution. So, starts with the wavenumber calculation.

4.2.1. Assumed Solution

Circular cylindrical shell model for analysis have boundary conditions of simply supported at y=0, W and free at s=0, 2L. From these boundary conditions, solution will be assumed with the form as

$$u = u_0 e^{-iks} \sin(\xi y) e^{iwt}, \tag{4.44}$$

$$v = v_0 e^{-iks} \cos(\xi y) e^{iwt} \tag{4.45}$$

and

$$w = w_0 e^{-iks} \sin(\xi y) e^{iwt}, \tag{4.46}$$

where k is s-directional wavenumber and ξ is y-directional wavenumber.

4.2.2. Spectrum Relation

Substituting of equation (4.44)-(4.46) into the governing equations (equation (4.41), (4.42) and (4.43)) gives the spectrum relation as

$$\begin{bmatrix} \alpha_1 - \left[k^2 + (1-\nu)\xi^2\right]\frac{D}{R^2} & \gamma & \left[\overline{E} + (k^2+\xi^2)D\right]\frac{ik}{R} \\ -\gamma & \alpha_2 & -\nu\overline{E}\frac{\xi}{R} \\ \left[\overline{E} + \left(k^2+\xi^2\right)D\right]\frac{ik}{R} & \nu\overline{E}\frac{\xi}{R} & \alpha_3 + \overline{E}\frac{1}{R^2} \end{bmatrix} \begin{Bmatrix} u_0 \\ v_0 \\ w_0 \end{Bmatrix} = 0 \quad , \tag{4.47}$$

where

$$\alpha_1 \equiv -\overline{E}\left[k^2 + \frac{1}{2}(1-\nu)\xi^2\right] + \rho h\omega^2 ,$$

$$\alpha_2 \equiv -\overline{E}\left[\xi^2 + \frac{1}{2}(1-\nu)k^2\right] + \rho h\omega^2 ,$$

$$\alpha_3 \equiv D\left[k^2 + \xi^2\right]^2 - \rho h\omega^2$$

and

$$\gamma \equiv \frac{1}{2}(1+\nu)\overline{E}ik\xi .$$

In the spectrum relation (equation (4.47)), in-plane (u_0, v_0) and out-of-plane

(w_0) wave displacements are coupled each other. This is a characteristic of cylindrical shell, which makes it harder to analyze than plate. Complexity from these coupling of displacements will be eliminated by making radius of curvature (R) infinity. This is shown as

$$\begin{bmatrix} \alpha_1 & \gamma & 0 \\ -\gamma & \alpha_2 & 0 \\ 0 & 0 & \alpha_3 \end{bmatrix} \begin{Bmatrix} u_0 \\ v_0 \\ w_0 \end{Bmatrix} = 0 . \tag{4.48}$$

It is same with the spectrum relation matrix for the plate. There is no coupling between in-plane and out-of-plane wave displacements.

4.2.3. Wave Number Calculation

To get solutions of equation (4.47), determinant of left hand side of matrix in equation (4.47) should be zero. The 8th order polynomial on k is presented as

$$a_1 k^8 + a_2 k^6 + a_3 k^4 + a_4 k^2 + a_5 = 0 , \tag{4.49}$$

where

$$a_1 = \frac{1}{2} \mathrm{D}\overline{\mathrm{E}}^2 - \frac{1}{2} \mathrm{D}\overline{\mathrm{E}}^2 \nu ,$$

$$a_2 = -\frac{D\bar{E}^2}{R^2} + \frac{D\bar{E}^2\nu}{R^2} - \frac{3}{2}D\bar{E}h\rho\omega^2 + \frac{1}{2}D\bar{E}h\nu\rho\omega^2 + 2D\bar{E}^2\xi^2$$
$$- 2D\bar{E}^2\nu\xi^2 + \frac{D^2\bar{E}\xi^2}{2R^2} - \frac{D^2\bar{E}\nu\xi^2}{R^2} + \frac{D^2\bar{E}\nu^2\xi^2 z^3}{2R^2},$$

$$a_3 = \frac{D\bar{E}^2}{2R^4} - \frac{D\bar{E}^2\nu}{2R^4} - \frac{1}{2}\bar{E}^2h\rho\omega^2 + \frac{1}{2}\bar{E}^2h\nu\rho\omega^2 + \frac{3D\bar{E}h\rho\omega^2}{2R^2}$$
$$+ \frac{D\bar{E}h\nu\rho\omega^2}{2R^2} + Dh^2\rho^2\omega^4 - \frac{3D\bar{E}^2\xi^2}{R^2} + \frac{2D\bar{E}^2\nu\xi^2}{R^2} + \frac{D\bar{E}^2\nu^2\xi^2}{R^2}$$
$$- \frac{9}{2}D\bar{E}h\rho\omega^2\xi^2 + \frac{3}{2}D\bar{E}h\nu\rho\omega^2\xi^2 - \frac{D^2h\rho\omega^2\xi^2}{R^2} + \frac{D^2h\nu\rho\omega^2\xi^2}{R^2}$$
$$+ 3D\bar{E}^2\xi^4 - 3D\bar{E}^2\nu\xi^4 + \frac{2D^2\bar{E}\xi^4}{R^2} - \frac{3D^2\bar{E}\nu\xi^4}{R^2} + \frac{D^2\bar{E}\nu^2\xi^4}{R^2},$$

$$a_4 = -\frac{D\bar{E}h\rho\omega^2}{R^4} - \frac{\bar{E}^2h\rho\omega^2}{2R^2} + \frac{\bar{E}^2h\nu\rho\omega^2}{2R^2} + \frac{3}{2}\bar{E}h^2\rho^2\omega^4 - \frac{1}{2}\bar{E}h^2\nu\rho^2\omega^4$$
$$+ \frac{Dh^2\rho^2\omega^4}{R^2} + \frac{3D\bar{E}^2\xi^2}{2R^4} - \frac{D\bar{E}^2\nu\xi^2}{R^4} - \frac{D\bar{E}^2\nu^2\xi^2}{2R^4} - \bar{E}^2h\rho\omega^2\nu^2$$
$$+ \bar{E}h\nu\rho\omega^2\xi^2 + \frac{D\bar{E}h\rho\omega^2\xi^2}{2R^2} + \frac{D\bar{E}h\nu\rho\omega^2\xi^2}{R^2} - \frac{D\bar{E}h\nu^2\rho\omega^2\xi^2}{2R^2}$$
$$+ 2Dh^2\rho^2\omega^4\xi^2 - \frac{2D\bar{E}^2\xi^4}{R^2} + \frac{D\bar{E}^2\nu\xi^4}{R^2} + \frac{D\bar{E}^2\nu^2\xi^4}{R^2} - \frac{9}{2}D\bar{E}h\rho\omega^2\xi^4$$
$$+ \frac{3}{2}D\bar{E}h\nu\rho\omega^2\xi^4 - \frac{2D^2h\rho\omega^2\xi^4}{R^2} + \frac{2D^2h\nu\rho\omega^2\xi^4}{R^2} + 2D\bar{E}^2\xi^6$$
$$- 2D\bar{E}^2\nu\xi^6 + \frac{5D^2\bar{E}\xi^6}{2R^2} - \frac{3D^2\bar{E}\nu\xi^6}{R^2} + \frac{D^2\bar{E}\nu^2\xi^6}{2R^2}$$

and

$$a_5 = \frac{\bar{E}h^2\rho^2\omega^4}{R^2} - h^3\rho^3\omega^6 - \frac{D\bar{E}h\rho\omega^2\xi^2}{R^4} + \frac{D\bar{E}h\nu\rho\omega^2\xi^2}{R^4} - \frac{3\bar{E}^2h\rho\omega^2\xi^2}{2R^2}$$
$$+ \frac{\bar{E}^2h\nu\rho\omega^2\xi^2}{2R^2} + \frac{\bar{E}^2h\nu^2\rho\omega^2\xi^2}{R^2} + \frac{3}{2}\bar{E}h^2\rho^2\omega^4\xi^2 - \frac{1}{2}\bar{E}h^2\nu\rho^2\omega^4\xi^2$$

$$+\frac{Dh^2\rho^2\omega^4\xi^2}{R^2}-\frac{Dh^2\nu\rho^2\omega^4\xi^2}{R^2}+\frac{D\bar{E}^2\xi^4}{R^4}-\frac{DE^2\nu\xi^4}{R^4}-\frac{D\bar{E}^2\nu^2\xi^4}{R^4}$$
$$+\frac{DE^2\nu^3\xi^4}{R^4}+\frac{\bar{E}^3\xi^4}{2R^2}-\frac{\bar{E}^3\nu\xi^4}{2R^2}-\frac{\bar{E}^3\nu^2\xi^4}{2R^2}+\frac{\bar{E}^3\nu^3\xi^4}{2R^2}-\frac{1}{2}\bar{E}^2h\rho\omega^2\xi^4$$
$$+\frac{1}{2}\bar{E}^2h\nu\rho\omega^2\xi^4-\frac{D\bar{E}h\rho\omega^2\xi^4}{R^2}+\frac{D\bar{E}h\nu\rho\omega^2\xi^4}{R^2}+Dh^2\rho^2\omega^4\xi^4$$
$$-\frac{3}{2}D\bar{E}h\rho\omega^2\xi^6+\frac{1}{2}D\bar{E}h\nu\rho\omega^2\xi^6-\frac{D^2h\rho\omega^2\xi^6}{R^2}+\frac{D^2h\nu\rho\omega^2\xi^6}{R^2}$$
$$+\frac{1}{2}D\bar{E}^2\xi^8-\frac{1}{2}D\bar{E}^2\nu\xi^8+\frac{D^2\bar{E}\xi^8}{R^2}-\frac{D^2\bar{E}\nu\xi^8}{R^2}.$$

The 8th order polynomial doesn't have analytic solution for the problem. So, to solve the equation, numerical mathematic solution program 'Mathematica' is used. And this numerical solution is very complicate to show in equation form. So, wavenumber that is obtained from numerical approach will be shown in the form of $k_1, k_2, k_3, \ldots$.

4.2.4. General Solution

Solution consists of eight wavenumber components. Since even number order polynomial exists only in equation (4.47), we can conclude that $k_1 = -k_5$, $k_2 = -k_6$, $k_3 = -k_7$, and $k_4 = -k_8$. So, the general solution can be expressed with wavenumbers as

$$\begin{aligned}\widetilde{u}(s) = {} & A_1 e^{-ik_1 s} + A_2 e^{-ik_2 s} + A_3 e^{-ik_3 s} + A_4 e^{-ik_4 s} \\ & + A_5 e^{-ik_1 (L-s)} + A_6 e^{-ik_2 (L-s)} + A_7 e^{-ik_3 (L-s)} + A_8 e^{-ik_4 (L-s)},\end{aligned} \tag{4.50}$$

where $A_1, A_2, \ldots, A_8$ is the amplitude and L is length of the shell in the hoop direction.

Also, similar expression for $\widetilde{v}$, $\widetilde{w}$ and $\widetilde{\psi}$ is valid. To simplify the expressions for displacements indicated above, it is interesting to think amplitude ratios between displacements as

$$\begin{Bmatrix} u_0 \\ v_0 \\ w_0 \\ \psi_0 \end{Bmatrix}_j = \begin{Bmatrix} 1 \\ \Omega_v \\ \Omega_w \\ \Omega_\psi \end{Bmatrix}_j u_0 = \{\Omega\}_j u_0, \tag{4.51}$$

where $\psi_0 = -ikw_0$ and the symbol Ω indicates amplitude ratio. Although the vector $\{\Omega\}$ is normalized with respect to u_0, it is possible for other nodal vectors to be normalized with different one. And amplitude ratio should be calculated for each mode k_j, hence there are eight vectors. These can be presented as

$$[\Omega] = [\,[\Omega_A],\ \ [\Omega_B]\,], \tag{4.52}$$

where

$$[\Omega_A] = \left[\begin{Bmatrix} 1 \\ \Omega_{v1} \\ \Omega_{w1} \\ \Omega_{\psi 1} \end{Bmatrix}_1 \quad \begin{Bmatrix} \Omega_{u2} \\ 1 \\ \Omega_{w2} \\ \Omega_{\psi 2} \end{Bmatrix}_2 \quad \begin{Bmatrix} \Omega_{u3} \\ \Omega_{v3} \\ 1 \\ \Omega_{\psi 3} \end{Bmatrix}_3 \quad \begin{Bmatrix} \Omega_{u4} \\ \Omega_{v4} \\ 1 \\ \Omega_{\psi 4} \end{Bmatrix}_4 \right]$$

and

$$[\Omega_B] = \left[\begin{Bmatrix} 1 \\ -\Omega_{v1} \\ -\Omega_{w1} \\ \Omega_{\psi 1} \end{Bmatrix}_1 \quad \begin{Bmatrix} -\Omega_{u2} \\ 1 \\ \Omega_{w2} \\ -\Omega_{\psi 2} \end{Bmatrix}_2 \quad \begin{Bmatrix} -\Omega_{u3} \\ \Omega_{v3} \\ 1 \\ -\Omega_{\psi 3} \end{Bmatrix}_3 \quad \begin{Bmatrix} -\Omega_{u4} \\ \Omega_{v4} \\ 1 \\ -\Omega_{\psi 4} \end{Bmatrix}_4 \right].$$

The $[4 \times 4]$ matrix $[\Omega_A]$ and $[\Omega_B]$ are evaluated at $+k_j$ and $-k_j$, respectively. And for each wavenumber k_j, Equation (4.52) gives the amplitude ratio among the displacements. To show it efficiently, simplify the variables of the spectrum relation matrix as

$$\begin{bmatrix} A1 & A2 & A3 \\ A4 & A5 & A6 \\ A7 & A8 & A9 \end{bmatrix} \begin{Bmatrix} u_0 \\ v_0 \\ w_0 \end{Bmatrix} = 0. \tag{4.53}$$

Calculation of any two equations in the spectrum relation (equation (4.53)) gives the amplitude ratio (equation (4.52)) as

$$\Omega_{v1} = \frac{(\mathrm{A1}\cdot\mathrm{A6} - \mathrm{A4}\cdot\mathrm{A3})}{(\mathrm{A5}\cdot\mathrm{A3} - \mathrm{A2}\cdot\mathrm{A6})},$$

$$\Omega_{w1} = \frac{(\mathrm{A1}\cdot\mathrm{A8} - \mathrm{A7}\cdot\mathrm{A2})}{(\mathrm{A9}\cdot\mathrm{A2} - \mathrm{A3}\cdot\mathrm{A8})},$$

$$\Omega_{\psi 1} = -ik\Omega_{w1},$$

$$\Omega_{u2} = \frac{(\mathrm{A5}\cdot\mathrm{A3} - \mathrm{A2}\cdot\mathrm{A6})}{(\mathrm{A1}\cdot\mathrm{A6} - \mathrm{A4}\cdot\mathrm{A3})},$$

$$\Omega_{w2} = \frac{(\mathrm{A5}\cdot\mathrm{A7} - \mathrm{A8}\cdot\mathrm{A4})}{(\mathrm{A9}\cdot\mathrm{A4} - \mathrm{A6}\cdot\mathrm{A7})},$$

$$\Omega_{\psi 2} = -ik\Omega_{w2},$$

$$\Omega_{u3} = \frac{(\mathrm{A9}\cdot\mathrm{A2} - \mathrm{A3}\cdot\mathrm{A8})}{(\mathrm{A1}\cdot\mathrm{A8} - \mathrm{A7}\cdot\mathrm{A2})},$$

$$\Omega_{v3} = \frac{(\mathrm{A9}\cdot\mathrm{A4} - \mathrm{A6}\cdot\mathrm{A7})}{(\mathrm{A5}\cdot\mathrm{A7} - \mathrm{A8}\cdot\mathrm{A4})},$$

$$\Omega_{\psi 3} = -ik,$$

$$\Omega_{u4} = \frac{(\mathrm{A9}\cdot\mathrm{A2} - \mathrm{A3}\cdot\mathrm{A8})}{(\mathrm{A1}\cdot\mathrm{A8} - \mathrm{A7}\cdot\mathrm{A2})},$$

$$\Omega_{v4} = \frac{(\mathrm{A9}\cdot\mathrm{A4} - \mathrm{A6}\cdot\mathrm{A7})}{(\mathrm{A5}\cdot\mathrm{A7} - \mathrm{A8}\cdot\mathrm{A4})}$$

and

$$\Omega_{\psi 4} = -ik\,. \qquad (4.54\text{-}4.65)$$

Now, displacement solution can be written as

$$\begin{aligned}\left\{\tilde{u}(s),\,\tilde{v}(s),\,\tilde{w}(s),\,\tilde{\psi}(s)\right\}^{T} &= \{U\}(s) \\ &= \{\Omega\}_1 A_1 e^{-ik_1 s} + \cdots + \{\Omega\}_8 A_8 e^{-ik_1(L-s)}\end{aligned}. \tag{4.66}$$

Using $[\Omega_A]$ and $[\Omega_B]$ in equation (4.52), the displacements can be shown in compact matrix form as

$$\{U\}(s) = [\Omega_A][e(s)]\{A\} + [\Omega_B][e(L-s)]\{B\}, \tag{4.67}$$

where the diagonal matrix of exponentials and the vector of amplitudes are given by

$$[e(s)] = \begin{bmatrix} e^{-ik_1 s} & 0 & 0 & 0 \\ 0 & e^{-ik_2 s} & 0 & 0 \\ 0 & 0 & e^{-ik_3 s} & 0 \\ 0 & 0 & 0 & e^{-ik_4 s} \end{bmatrix},$$

$$\{A\} = \begin{Bmatrix} A_1 \\ A_2 \\ A_3 \\ A_4 \end{Bmatrix} \quad \text{and} \quad \{B\} = \begin{Bmatrix} A_5 \\ A_6 \\ A_7 \\ A_8 \end{Bmatrix}.$$

4.2.5. Nodal Displacements

It is necessary to replace the vectors $\{A\}$ and $\{B\}$ in equation (4.67) in terms of the nodal displacements at s=0 and s=L. That is

$$\tilde{u}(0) = \tilde{u}_1,\ \tilde{v}(0) = \tilde{v}_1,\ \ \tilde{w}(0) = \tilde{w}_1 \ and\ \ \tilde{\psi}(0) = \tilde{\psi}_1 \qquad (4.68)$$

with similar terms at s=L. Write this in matrix notation as

$$\begin{Bmatrix} \{\tilde{u}\}_1 \\ \{\tilde{u}\}_2 \end{Bmatrix} = \begin{bmatrix} [\Omega_A][e(0)]\{A\} & [\Omega_B][e(L)]\{B\} \\ [\Omega_A][e(L)]\{A\} & [\Omega_B][e(0)]\{B\} \end{bmatrix} \begin{Bmatrix} \{A\} \\ \{B\} \end{Bmatrix}. \qquad (4.69)$$

where,

$$\{\tilde{u}_1, \tilde{v}_1, \tilde{w}_1, \tilde{\psi}_1\}^T = \{\tilde{u}\}_1 = \{U\}(0) = [\Omega_A][e(0)]\{A\} + [\Omega_B][e(L)]\{B\},$$

and

$$\{\tilde{u}_2, \tilde{v}_2, \tilde{w}_2, \tilde{\psi}_2\}^T = \{\tilde{u}\}_2 = \{U\}(L) = [\Omega_A][e(L)]\{A\} + [\Omega_B][e(0)]\{B\}.$$

Solving for the coefficients gives

$$\begin{Bmatrix}\{A\}\\ \{B\}\end{Bmatrix}=\begin{bmatrix}[\Omega_A][e(0)]\{A\} & [\Omega_B][e(L)]\{B\}\\ [\Omega_A][e(L)]\{A\} & [\Omega_B][e(0)]\{B\}\end{bmatrix}^{-1}\begin{Bmatrix}\{\widetilde{u}\}_1\\ \{\widetilde{u}\}_2\end{Bmatrix}$$

$$=[G]\begin{Bmatrix}\{\widetilde{u}_1\}\\ \{\widetilde{u}_2\}\end{Bmatrix}=\begin{bmatrix}[G_{11}] & [G_{12}]\\ [G_{21}] & [G_{22]}\end{bmatrix}\begin{Bmatrix}\{\widetilde{u}_1\}\\ \{\widetilde{u}_2\}\end{Bmatrix}, \tag{4.70}$$

where each partition of [G] is of size [4 × 4]. Finally, the displacements will be shown in terms of the shape functions by replacing {A} and {B} in equation (4.67) with equation (4.70) as

$$\{U\}(s)=[g(s)]_1\{\widetilde{u}\}_1+[g(s)]_2\{\widetilde{u}\}_2, \tag{4.71}$$

where the [4 × 4] matrix of shape functions are defined as

$$[g(s)]_1=[\Phi_A][e(s)][G_{11}]+[\Phi_B][e(L-s)][G_{21}]$$

and

$$[g(s)]_2=[\Phi_A][e(s)][G_{12}]+[\Phi_B][e(L-s)][G_{22}].$$

4.2.6. Nodal Forces

Spectral stiffness matrix requires two components to be defined in force-displacement relation. General displacement is defined above. For the next step,

forces on the element boundary should be considered. Since the boundary conditions (Equation (4.37)-(4.40)) are already derived using Hamilton's principle, it is necessary to connect those with resultants. Resultants per unit length for shell segment are

$$N_{ss} \equiv \int \sigma_{ss} dz \tag{4.72}$$

and

$$N_{sy} \equiv \int \sigma_{sy} dz \,. \tag{4.73}$$

After substituting for the stresses and strains in terms of our approximations leads to

$$N_{ss} = \overline{E}\left[\frac{\partial u}{\partial s} - \frac{w}{R} + \nu \frac{\partial v}{\partial y}\right] \tag{4.74}$$

and

$$N_{sy} = \frac{1}{2}(1-\nu)\overline{E}\left[\frac{\partial v}{\partial s} + \frac{\partial u}{\partial y}\right]. \tag{4.75}$$

And resultant moments per unit length for shell segment are

$$M_{ss} = -\int \sigma_{ss} z dz \tag{4.76}$$

and

$$M_{sy} = -\int \sigma_{sy} z dz . \tag{4.77}$$

Again, after substituting for the stresses and strains in terms of our approximations leads to

$$M_{ss} = D\left[\frac{\partial^2 w}{\partial s^2} + \frac{1}{R}\frac{\partial u}{\partial s} + \nu \frac{\partial^2 w}{\partial y^2}\right] \tag{4.78}$$

and

$$M_{sy} = \frac{1}{2} D(1-\nu)\frac{\partial}{\partial y}\left[\frac{u}{R} + 2\frac{\partial w}{\partial s}\right]. \tag{4.79}$$

Comparing these expressions to those for the boundary conditions, the natural boundary conditions are equivalent to specifying

$$Q_u = N_{ss} + \frac{1}{R} M_{ss},$$

$$Q_v = N_{sy},$$

$$Q_w = -\frac{\partial M_{ss}}{\partial s} - \frac{\partial M_{sy}}{\partial y} = V_{sz}$$

and

$$Q_m = M_{ss}\,. \qquad (4.80\text{-}4.83)$$

4.2.7. Spectral Element Matrix

From calculated displacements and forces above, it is possible to derive stiffness relation for the shell segment. The process is simply that of expressing the resultant forces and moments in terms of the displacement solutions given in equation (4.71):

$$F(s) = \left\{ N_{ss} + \frac{1}{R} M_{ss},\ N_{sy},\ V_{sz},\ M_{ss} \right\}^T (s) = [\partial]\{U\}(s), \qquad (4.84)$$

where $[\partial]$ is the matrix collection of differential operators of size [4 $\times$ 4]. After substituting for $\{U\}(s)$ in terms of the shape functions, equation (4.84) becomes

$$\{F\}(s) = [\partial][g(s)]_1 \{\tilde{u}\}_1 + [\partial][g(s)]_2 \{\tilde{u}\}_2 \qquad (4.85)$$

$$= [\partial g(s)]_1 \{\tilde{u}\}_1 + [\partial g(s)]_2 \{\tilde{u}\}_2\,.$$

Relating the member resultants at s=0 and s=L to the nodal loads at the same locations leads to the stiffness relation:

$$\begin{Bmatrix} \{\widetilde{F}\}_1 \\ \{\widetilde{F}\}_2 \end{Bmatrix} = \begin{bmatrix} [-\partial g(0)]_1 & [-\partial g(0)]_2 \\ [+\partial g(L)]_1 & [+\partial g(L)]_2 \end{bmatrix}, \tag{4.86}$$

where

$$\{\widetilde{F}\} \equiv \{\widetilde{N}_1, \widetilde{F}_{y1}, \widetilde{V}_1, \widetilde{M}_1; \ \widetilde{N}_2, \widetilde{F}_{y2}, \widetilde{V}_2, \widetilde{M}_2\}^T$$

and

$$\{\widetilde{u}\} \equiv \{\widetilde{u}_1, \widetilde{v}_1, \widetilde{w}_1, \widetilde{\psi}_1; \widetilde{u}_2, \widetilde{v}_2, \widetilde{w}_2, \widetilde{\psi}_2\}^T \quad .$$

Equation (4.86) is the simplest form of matrix when the structure has one element. But for the structural vibration analysis, the structure consists of element more than one in general. As mentioned in earlier chapter, the spectral finite element method has the number of element, which is divided at the point of impedance changing. In our case, shell model has two elements because external force is applied at center of cylindrical shell (s=L) in s-direction. (See Fig. 4.4) Then stiffness relation becomes

$$\begin{Bmatrix} \{\widetilde{F}\}_1 \\ \{\widetilde{F}\}_2 \\ \{\widetilde{F}\}_3 \end{Bmatrix} = \begin{bmatrix} [-\partial g(0)]_1 & [-\partial g(0)]_2 & zeros(4,4) \\ [+\partial g(L)]_1 & [+\partial g(L)]_2 + [-\partial g(0)]_1 & [-\partial g(0)]_2 \\ zeros(4,4) & [+\partial g(L)]_1 & [+\partial g(L)]_2 \end{bmatrix}, \quad (4.87)$$

where zeros(4,4) is zero matrix of size [4 × 4].

But unlike structural vibration analysis that analyze only at the center points of the shell (s=L, y=W/2), the radiated noise analysis focuses on many points. So, in the case of radiated noise analysis, shell model consists of 3 elements. Then, stiffness relation becomes

$$\begin{Bmatrix} \{\widetilde{F}\}_1 \\ \{\widetilde{F}\}_2 \\ \{\widetilde{F}\}_3 \\ \{\widetilde{F}\}_4 \end{Bmatrix} = \begin{bmatrix} [-\partial g(0)]_1 & [-\partial g(0)]_2 & zeors(4,4) & zeors(4,4) \\ [+\partial g(L1)]_1 & [+\partial g(L1)]_2 + [-\partial g(0)]_3 & [-\partial g(0)]_4 & zeors(4,4) \\ zeros(4,4) & [+\partial g(L2)]_3 & [+\partial g(L2)]_4 + [-\partial g(0)]_5 & [-\partial g(0)]_6 \\ zeros(4,4) & zeros(4,4) & [+\partial g(L3)]_5 & [+\partial g(L3)]_6 \end{bmatrix}, \quad (4.88)$$

where the subscript number 1, 2, 3, 4, 5, 6 are node number and L1, L2, L3 are the s-directional length of the element.

4.3. Indirect BEM for Cylindrical Shell

4.3.1. Equations of Indirect BEM

To apply the boundary element method in open sound field, indirect boundary element method needs to be considered. Formulation of the indirect boundary element method can be shown as

$$p(x) = \int_{\partial\Omega} G(x,\xi)\phi(\xi)d\partial\Omega + \int_{\Omega} G(x,z)\Psi(z)d\Omega \qquad (4.89)$$

and

$$\begin{aligned} u(x) &= -\frac{\partial p}{\partial n} \\ &= \int_{\partial\Omega} F(x,\xi)\phi(\xi)d\partial\Omega + \int_{\Omega} F(x,z)\Psi(z)d\Omega, \end{aligned} \qquad (4.90)$$

where $\partial\Omega$ is boundary surface, $G(x,\xi)$ is Green's function, $F(x,\xi)$ is derivative of Green's function with normal direction to the surface, x is field point, ξ is virtual source point and z is real source point.

Because there is no input source in our shell model for the radiated noise analysis, the last term for the real source in equation (4.89) and (4.89) can be excluded for the process. So, Those are

$$p(x) = \int_{\partial\Omega} G(x,\xi)\phi(\xi)d\partial\Omega \tag{4.91}$$

and

$$\begin{aligned} u(x) &= -\frac{\partial p}{\partial n} \\ &= \int_{\partial\Omega} F(x,\xi)\phi(\xi)d\partial\Omega. \end{aligned} \tag{4.92}$$

Starts from equation (4.91) and (4.92), there are four things that should be covered in this section. Those are Green's function, displacement input, Gauss quadrature and Cauchy principle value: First, Green's function is a essential part of boundary element method that governs the pressure field what we want to find. Second, displacements from the structural vibration analysis are used for an input in the boundary element method. Originally, normal velocity on the surface is an input for the boundary element method. Third, the Gauss quadrature is convenient to integrate on the domain of arbitrary shape of surface. And fourth, Cauchy principle value is the treatment of singular error, which is occurs when field point indicates the same position with virtual source point in the integration process. Fig. 4.4 shows how those works in the entire process.

4.3.2. Green's Function

A Green's function is a type of function used to solve inhomogeneous differential equations subject to boundary conditions. Greens function that governs the open sound field is expressed in the form of exponential function with length between x and ξ as

$$G(x,\xi) = \frac{1}{4\pi}\frac{e^{-jkr}}{r} \tag{4.93}$$

and

$$F(x,\xi) = -\frac{\partial G}{\partial n} = \frac{(jkr+1)}{4\pi r^3} e^{-jkr} r_i n_i, \tag{4.94}$$

where $r = |x-\xi|$.

4.3.3. Displacements Input

As mentioned, displacements from the structural vibration analysis are the inputs for radiated noise analysis. But only out-of-plane wave displacement is used for the radiated noise analysis because that in-plane wave displacement is not effective at radiation of noise. Since velocity is generally used in analysis of the BEM (equation (4.91) and (4.92)), displacements should be transformed based on the Euler equation with an assumption of time harmonic function. So, that is

$$\begin{aligned}\nabla p &= -\rho \frac{\partial v}{\partial t} \\ &= -\, j\omega\rho v \\ &= \omega^2 \rho w\,,\end{aligned} \tag{4.95}$$

where ρ is density of structure and ω is frequency for analysis. And relation between pressure and displacement, which are normal to the surface, is shown as

$$\frac{\partial p}{\partial n} = \nabla p \cdot n_i = \omega^2 \rho_0 w \cdot n_i = \omega^2 \rho_0 w_n\,. \tag{4.96}$$

4.3.4. Solution Obtaining Procedure

Putting equation (4.95) and (4.96) into general indirect BEM equation (equation (4.91) and (4.92)) gives the equation as

$$-\rho\omega^2 w = \int_{\partial\Omega} \frac{(jkr+1)}{4\pi r^3} e^{-jkr} r_i n_i \phi(\xi) d\partial\Omega\,, \tag{4.97}$$

where i indicate boundary element point. $i = 1,2,3....$

For the next step, virtual source value needs to be calculated from Equation (4.97). So, the Gauss quadrature is used for integration. The Gauss quadrature is

an approximation of the definite integral of a function, usually stated as a weighted sum of function values at specified points within the domain of integration. Specifically two Gauss points are used for radiated noise analysis of cylindrical shell. But while do the integration using the Gauss quadrature, singular can be occurred at the point that has zero value of length between field point and virtual source point ($r = |x - \xi|$). So, to prevent singular in the integration process, the Cauchy principle value at the singular point is used. And in our case, 0.5 is used as the Cauchy principle value because surface of cylindrical shell is smooth. Then, equation (4.97) becomes

$$\begin{aligned} u(x_0) &= \int_{\partial\Omega} F(x_0, \xi)\phi(\xi) dS(\xi) \\ &= -\frac{1}{2}\phi(x_0) + \int_{\partial\Omega - 0} F(x_0, \xi)\phi(\xi) dS(\xi), \end{aligned} \tag{4.98}$$

where x_0 is a singular point, $\partial\Omega - 0$ is surface domain without singular points in. After calculating the virtual source value, it is possible to derive the equation for pressure, which is

$$p(x) = \int_{\partial\Omega} \left(\frac{1}{4\pi} \frac{e^{-jkr}}{r} \right) \phi(\xi)\, d\partial\Omega . \tag{4.99}$$

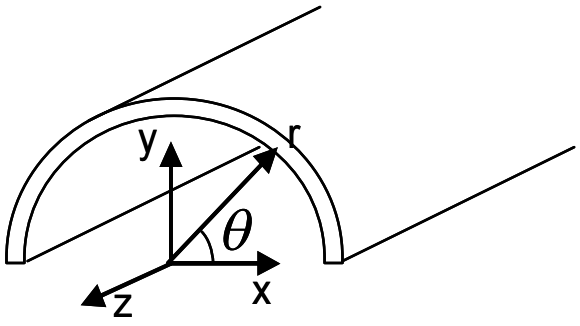

Fig. 4.1 Circular cylindrical coordinates (x, y and z are rectangular coordinates axis; r, θ and z are cylindrical coordinates axis)

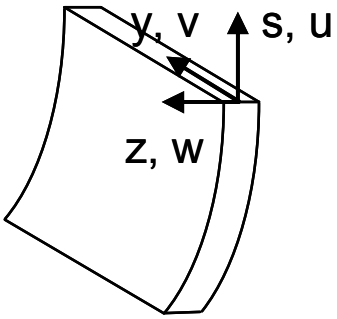

Fig. 4.2 Shell based coordinates (s, y and z are shell based coordinates axis; u, v and w are displacements)

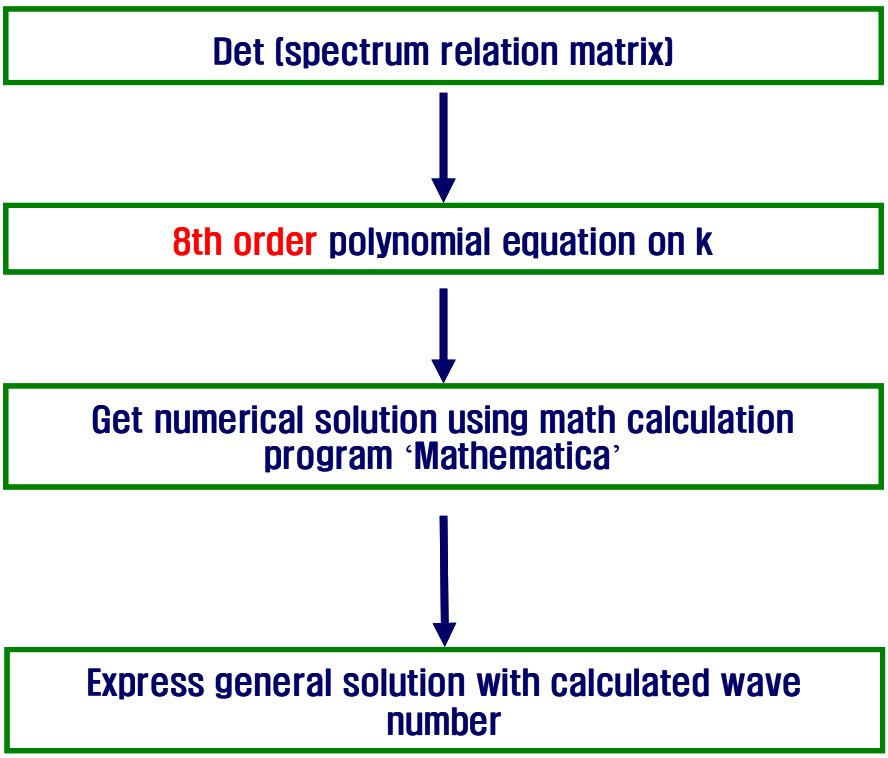

Fig. 4.3 S-directional wavenumber 'k' calculation procedures

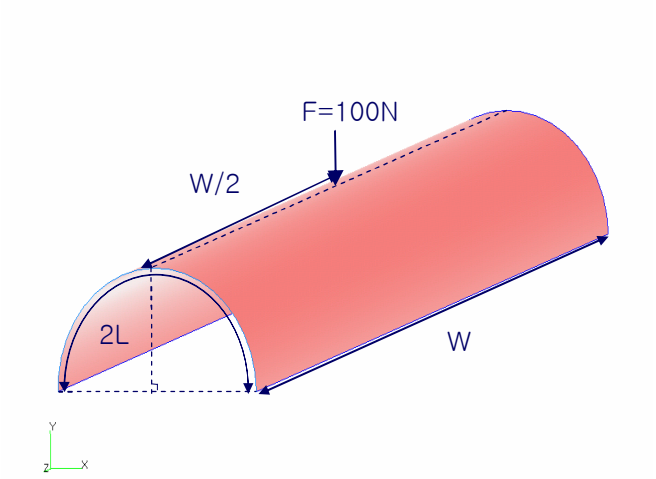

Fig. 4.4 Shell model for the structural vibration analysis

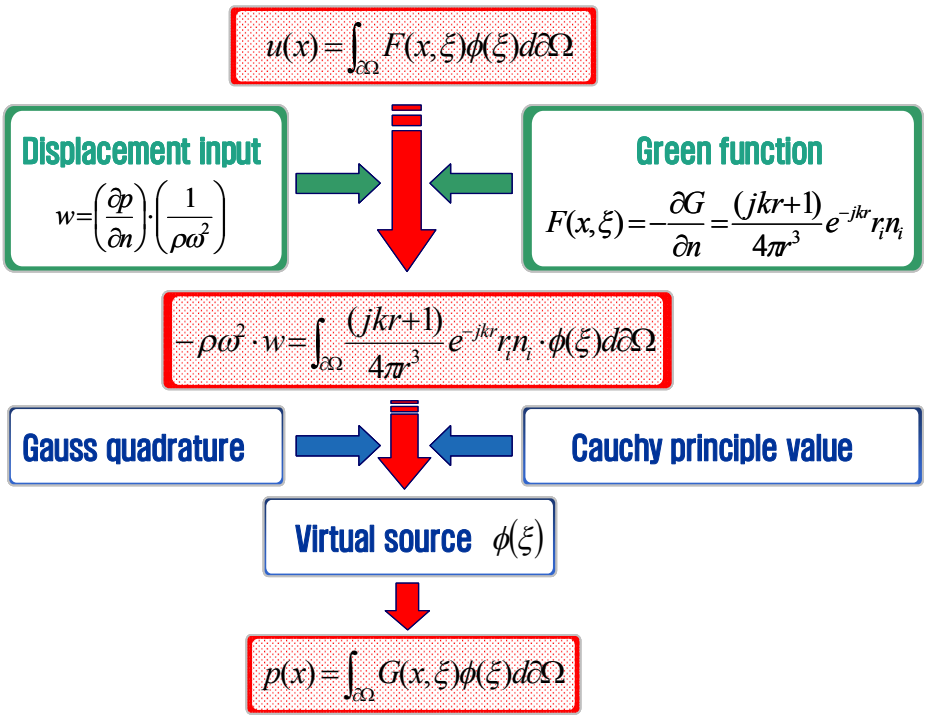

Fig. 4.5 Indirect BEM procedures

5. Results and Discussion

5.1. Structural Vibration Analysis

Structural vibration analysis was carried out using a circular cylindrical shell model for simply supported boundary conditions on y=0, W and free boundary conditions on s=0, 2L. And radius of the shell was 1m, total length in the y-direction was 15m and the applied force was set to 100N. (See Fig. 5.1) Details of the property of the shell model are shown in Table. 5-1.

As mentioned, the number of elements used by the spectral finite element method is determined by the impedance changing part in the structure. In Fig. 5.1, an external force that is applied at the center of the shell model in the s-direction is shown. Therefore, only one impedance changing part exists in the shell model; consequently, the shell model used for the structural vibration analysis has just two elements. Naturally, the total node number is 3 for the analysis.

The analysis gave the frequency response function, which is defined as the ratio of out-of-plane wave displacements and external force in the frequency domain. Since the spectral finite element method is applied in the frequency domain, the results from the analysis are also frequency dependent values. Therefore, the frequency response function is appropriate for showing the results. Of course,

displacements and external forces are transformed to the frequency domain with FFT (Fast Fourier Transforms).

$$FRF(s,\omega) = \log_{10}\left(\frac{w(s,\omega)}{F(\omega)}\right) \qquad (5.1)$$

where, ω is the frequency used in the analysis.

To verify the results of the structural vibration analysis with the spectral finite element method, the commercial program 'NASTRAN', which is based on the finite element method, is used. The FEM shell model has 25,920 elements, and uses all the same conditions (boundary condition, external force) that were used in the shell model for the spectral finite element method (Fig. 5.1). The FEM shell model is shown in Fig. 5.2.

The results of the spectral finite element method model and finite element method model (25,920 elements) were compared for the frequency domain of 0 to 300Hz. (See Fig. 5.3) Fig. 5.3 shows that the results between spectral finite element method model and finite element method model (25,920 elements) match well. But specifically, different pattern between two models is gradually shown when analysis frequency increases beyond 100Hz. This difference in the 100~300 Hz frequency range comes from a shortfall of the FEM, which uses a static shape

function.

To find out the details of this difference, the results obtained from a set of FEM models of different number of elements (1,620, 6,480, and 14,580) were compared with the results from the spectral finite element method model. Fig. 5.4 shows that the results from both types of models are almost well matched in the 0 to 50Hz frequency range. But the FEM model having 1,620 elements contained error in the frequency range above 30Hz. Another case of comparison is shown in Fig. 5.5 in the frequency range of 150 to 200Hz. In this figure, the results from the FEM models with 1,620 and 6,480 elements, respectively, showed poor accuracy, and the results from the FEM model with 14,580 elements showed reasonable accuracy. From this comparison, it is natural to conclude that FEM needs sufficient number of elements to give reasonable accuracy. Moreover, as the analysis frequency increases, more elements are needed.

Increasing the number of elements means the increase of analysis running time. Therefore, it is meaningful to see how much time it takes to analyze with SFEM and FEM for different numbers of elements. Basically, SFEM of 2 and FEM of 25,920 elements model are compared in Fig. 5.3. The FEM model of 25,920 elements gave reasonable accuracy in the frequency band of 0 to 300Hz. Operation time for SFEM and FEM model is suggested in Table. 5-2: the SFEM model of 2 elements took 373 seconds and the FEM model of 25,920 elements

took 8,635 seconds. The operation time of the FEM model, normalized by the SFEM operation time, was 23 times longer than that of SFEM model. This is a big difference between the two methods, and this difference becomes huge when the analysis frequency increases far beyond 300Hz.

As mentioned in an earlier chapter, SFEM uses a frequency dependent shape function and FEM uses a frequency independent shape function. Therefore, SFEM does not have to change the number of elements it uses, whatever the analysis frequency is, unlike the FEM, which needs to change the number of elements according to the analysis frequency. Fig. 5.6 shows the advantage of the SFEM model over the FEM model with respect to the operation time. Only the FEM model with 1,620 numbers of elements took less operation time than the SFEM model, but it could not predict a frequency response function beyond 50Hz, as shown in Fig. 5.4. The operation times of the FEM models of 6,480, 14,580 and 25,920 elements were 1,312, 4,117 and 8,635, respectively. To compare values of the operation times between the two types of models, it is good to normalize them by the SFEM operation time. After normalizing, the operation times of the FEM models indicated above were 3.5, 11 and 23, respectively. Therefore, the SFEM formulation of the shell model showed two distinct advantages: one, SFEM formulation can give an accurate result, regardless of analysis frequency and two, with respect to operation time. SFEM formulation

requires the same operation time at any frequency band. These advantages will make a big difference with respect to analysis performances when the analysis frequency is in the high frequency range.

Based on the verification of the results of the SFEM model, structural vibration analysis was also performed in the mid- and high- frequency ranges. This analysis showed that SFEM formulation can give fast and reliable results in the high frequency range. (See Fig. 5.7)

5.2. Radiated Noise Analysis

Radiated noise analysis was carried out using the indirect boundary element method. In the general indirect BEM equation, the velocities at the surface of a structure are used as an input to obtain pressures at the field points. But the spectral finite element method formulation of a circular cylindrical shell provides displacements at the surface of the structure. As mentioned in section 4.3, coupling factors are needed to use the results from the structural vibration analysis that is formulated with SFEM. So, based on the assumption of a harmonic wave, displacements are transformed to adequate form (= derivative of pressure with normal vector) using the Euler equation.

A circular cylindrical shell model for structural vibration analysis was also used for radiated noise analysis. But unlike the structural vibration analysis that fixes a field point at one specific boundary point, radiated noise analysis focuses on many field points. The field for analysis is presented as a form of a rectangular plate above the circular cylindrical shell. (See Fig. 5.8) The plate has dimensions of 15m in length in the y-direction and 2m in width in the x-direction.

The reliability of the results of radiated noise analysis is verified by comparisons of the results with those given by the commercial tool 'SYSNOISE'. Since SYSNOISE program are based on the indirect boundary element method, it is

natural to conclude that both cases (= one is indirect BEM coding using Matlab, the other is SYSNOISE) use the same analysis method. But the difference between the two cases is the input value. Indirect BEM coding uses the displacements from the SFEM formulation, whereas SYSNOISE uses the displacements from NASTRAN (=commercial tool that is based on FEM). To set the same analysis conditions, the shell model and field points for SYSNOISE are set the same as those for Indirect BEM coding. Details of the property are shown in Table. 5-3.

Boundary segmentation is essential to analyze the radiated noise using boundary element method. And boundary segmentation is related with the maximum analysis frequency. Basically, six elements per wavelength is required at the frequency of analysis to obtain reliable results in BEM. So, maximum frequency increases with progression of boundary segmentation. In this analysis, 1,620 element segmentation was performed and this condition was the same in the SYSNOISE analysis.

The frequency for analysis is selected by considering the FEM operation time. As mentioned, FEM requires long operation time and gives error-contained results when the analysis frequency increases. Therefore, the analysis frequency was selected in the low frequency range. But very low (=below 20Hz) analysis frequency can give inaccurate results because radiated noise analysis with SFEM

uses only out-of-plane displacement wave components as an input. In the mid- and high- frequency range, this input is reasonable based on the assumption that out-of-plane wave components are the most effective noise radiation factor. But the membrane effect is dominating in the very low frequency range. In other words, in-plane-wave components also need to be considered in that frequency range.

Based on the above, analysis frequency was selected as 30, 50, and 90Hz. And the results are shown in Fig. 5.9, Fig. 5.10, and Fig. 5.11, respectively. But it is hard to compare the two results numerically from these figures. So, a centerline comparison is presented in Fig. 5.12, Fig. 5.13, and Fig. 5.14. Centerline is located at the center of x-axis (x=0) and extend from y=0 to y=15. From these results, it is natural to conclude that radiated noise analysis with SFEM gives accurate results.

The maximum analysis frequency for indirect BEM and SYSNOISE is the same because both cases have the same boundary segmentation. And this maximum frequency is higher than 150Hz for our analysis model. Now, it is meaningful to check the accuracy of the results for both cases. Fig. 5.15 indicates the frequency response function of the FEM models of 1,620, 6,480, and 14,580 and SFEM in the frequency range of 85Hz ~ 135Hz. At the frequency 127Hz, the result of 1,620 element FEM model showed inaccurate value because the FEM did not

have enough elements to give accurate results. The 1,620 element FEM model could not give accurate results at the frequency 127Hz even though the frequency was within the maximum analysis frequency of BEM. But indirect BEM formulation with SFEM gave accurate results within the maximum frequency range because SFEM provides accurate results independent of the frequency range, as shown in Fig. 5.16 and Fig. 5.17.

Therefore, SFEM for the radiated noise analysis gives more accurate results within the maximum frequency range than FEM.

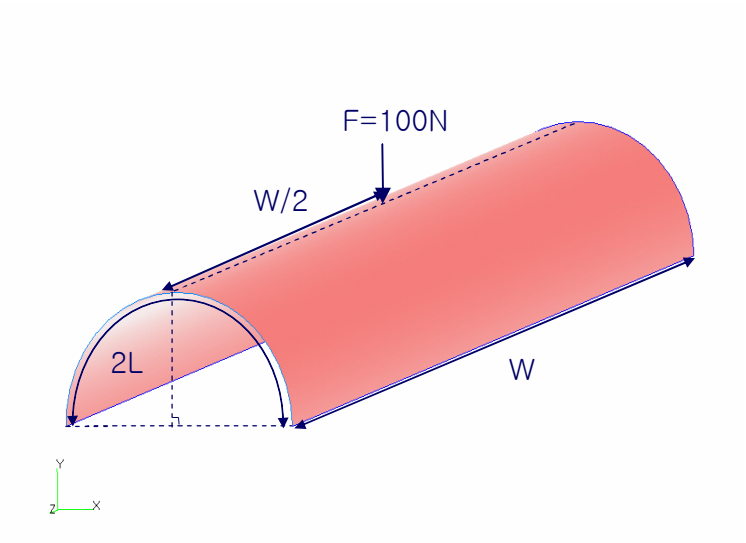

Fig. 5.1 Shell model for the structural vibration analysis; simply supported boundary conditions on y=0, W and free boundary conditions on s=0, 2L

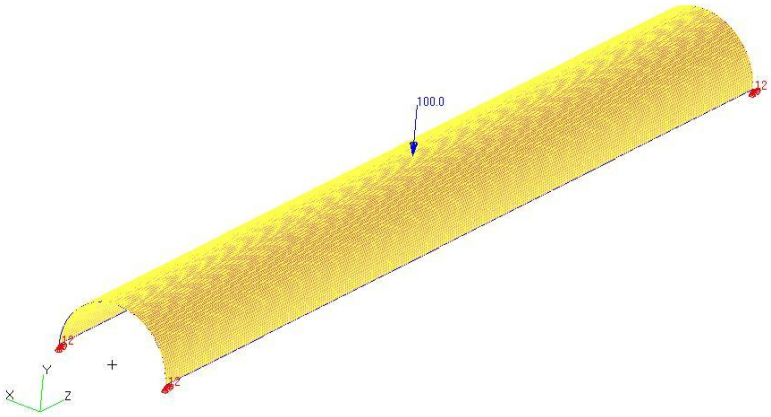

Fig. 5.2 Shell model for the FEM (finite element method) analysis

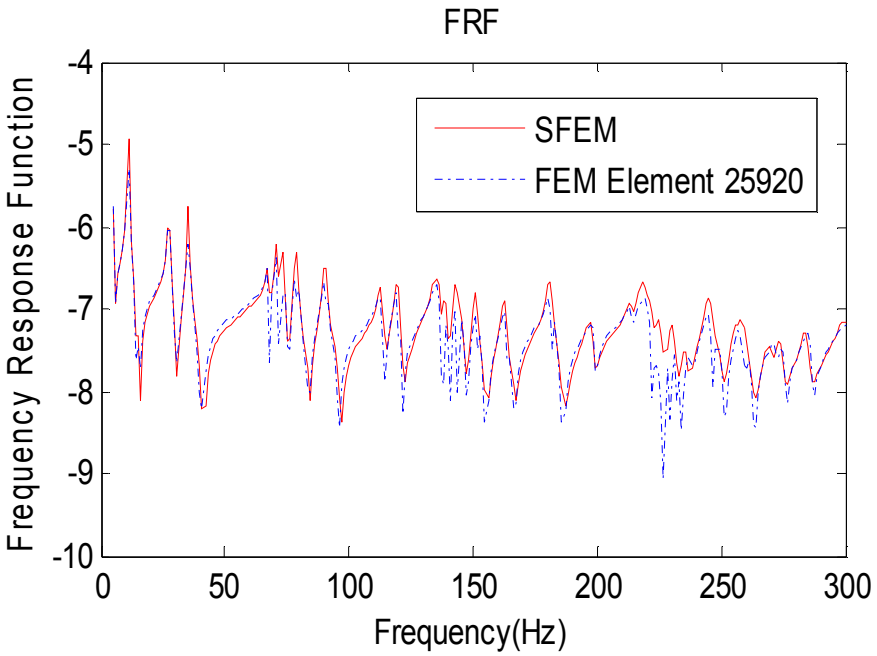

Fig. 5.3 Comparison of the frequency response function (FRF) between the SFEM model and the FEM model (25920 elements) of circular cylindrical shell

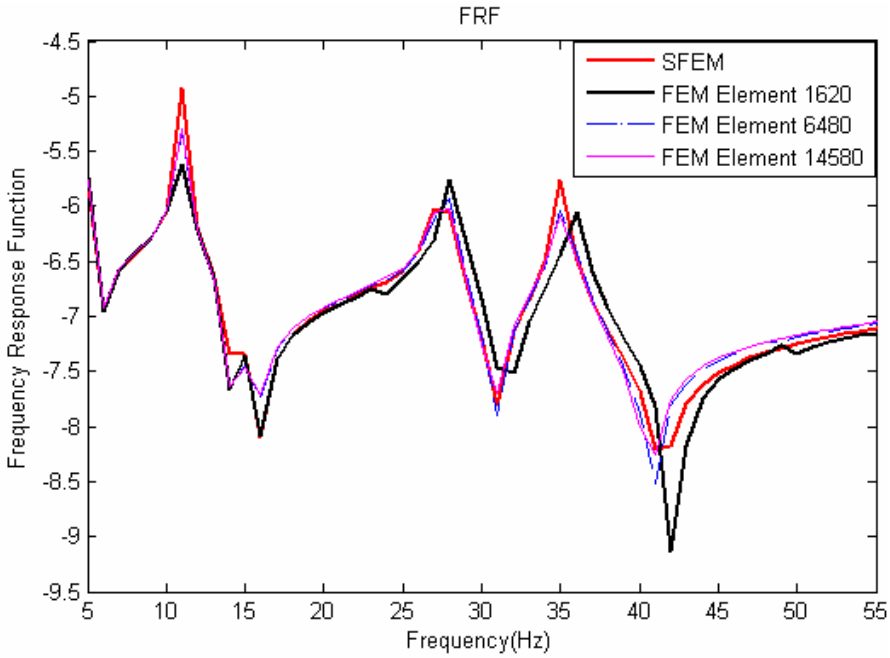

Fig. 5.4 Comparison of the SFEM and the FEM with different number of element at 5~50Hz

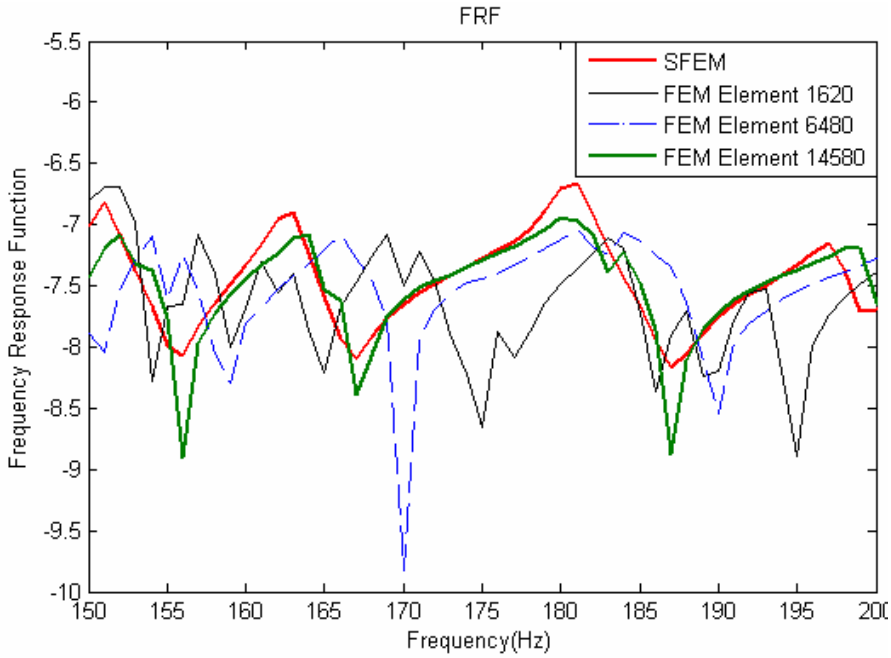

Fig. 5.5 Comparison of SFEM and FEM with different number of element at 150~200Hz

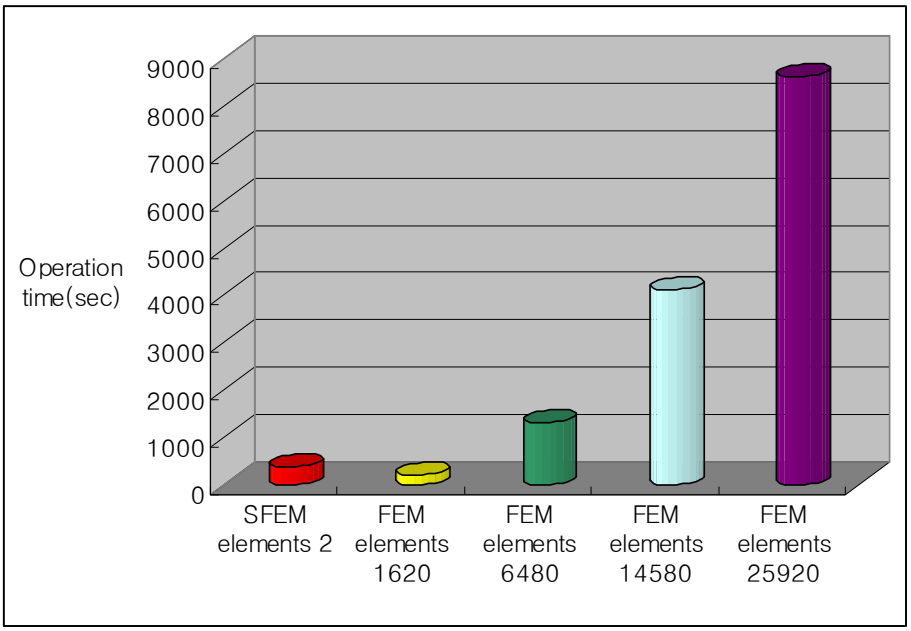

Fig. 5.6 Operation time for the SFEM and the FEM

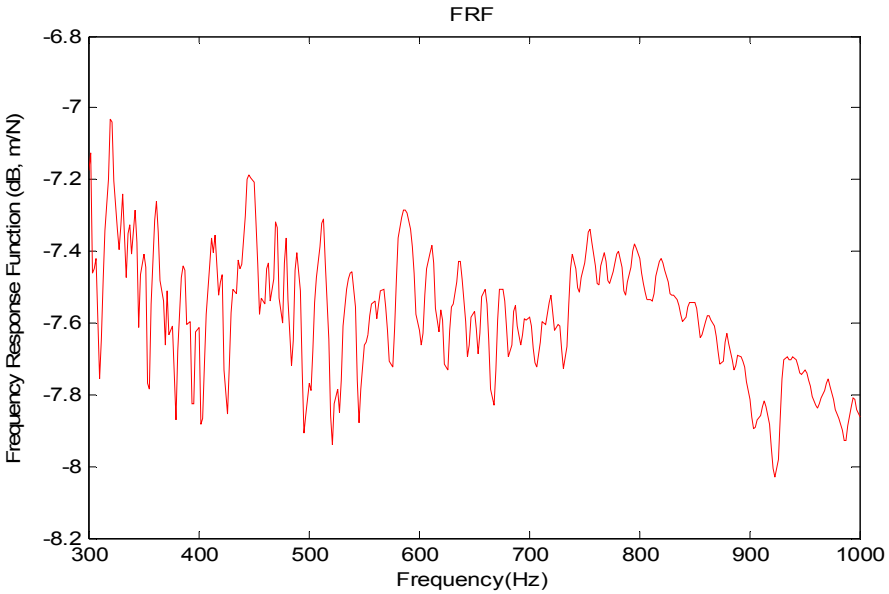

Fig. 5.7 Frequency response function for mid- and high- frequency range (300 ~ 1000Hz)

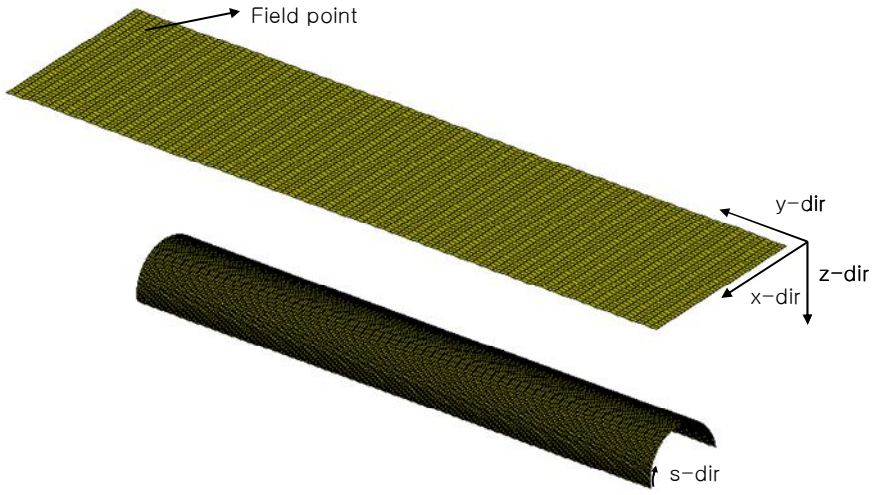

Fig. 5.8 Shell model and the field points for radiated noise levels

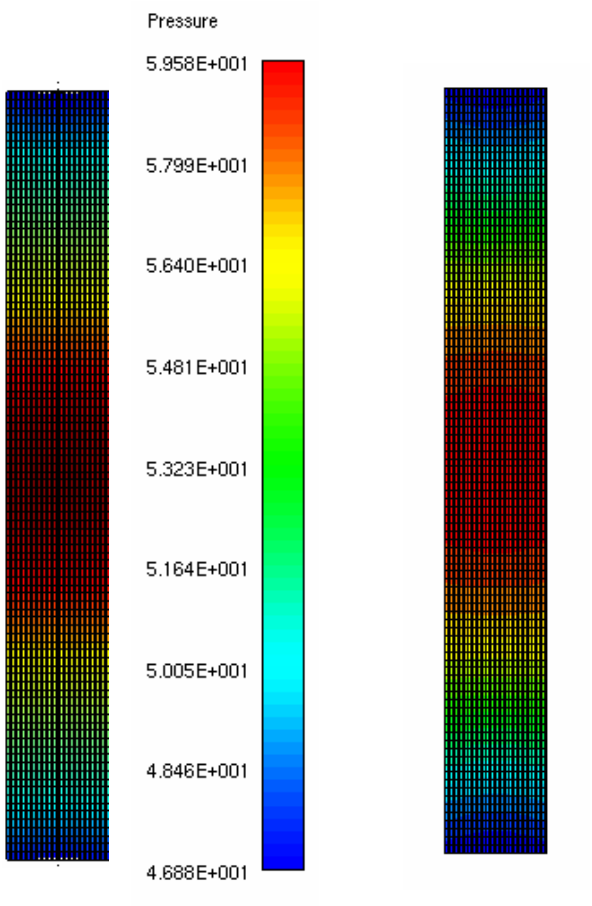

Fig. 5.9 Radiated noise level (dB) at 30Hz:
Matlab coding using indirect BEM (left hand side),
SYSNOISE program (right hand side)

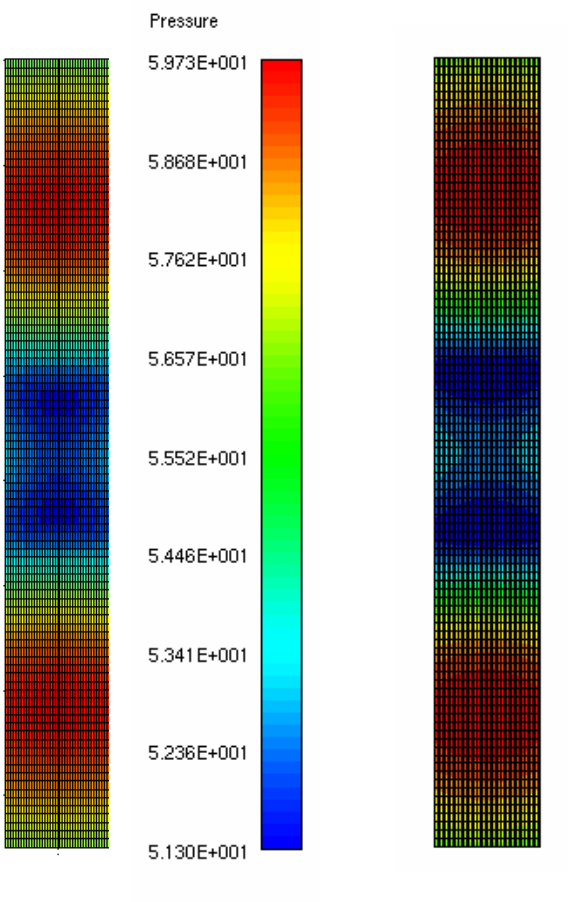

Fig. 5.10 Radiated noise level (dB) at 50Hz:
Matlab coding using indirect BEM (left hand side),
SYSNOISE program (right hand side)

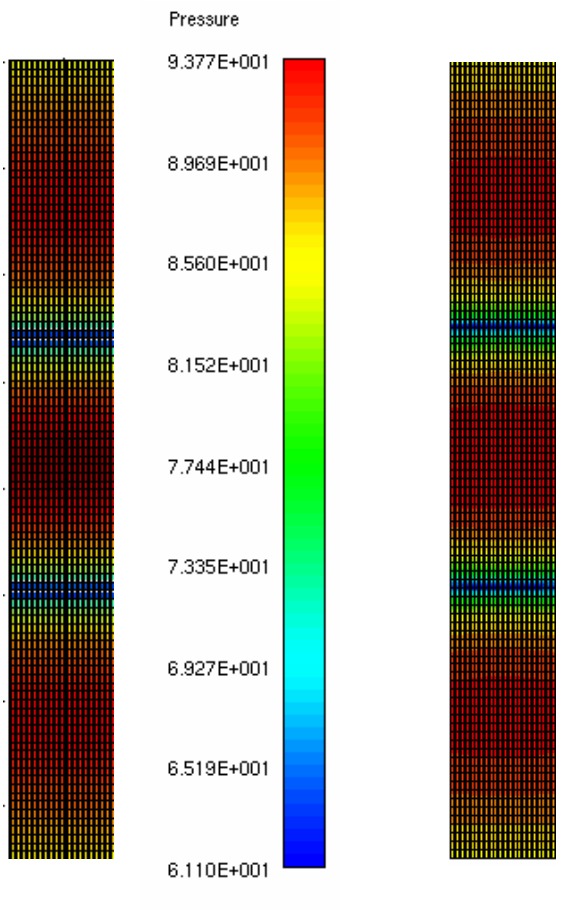

Fig. 5.11 Radiated noise level (dB) at 90Hz:
Matlab coding using indirect BEM (left hand side),
SYSNOISE program (right hand side)

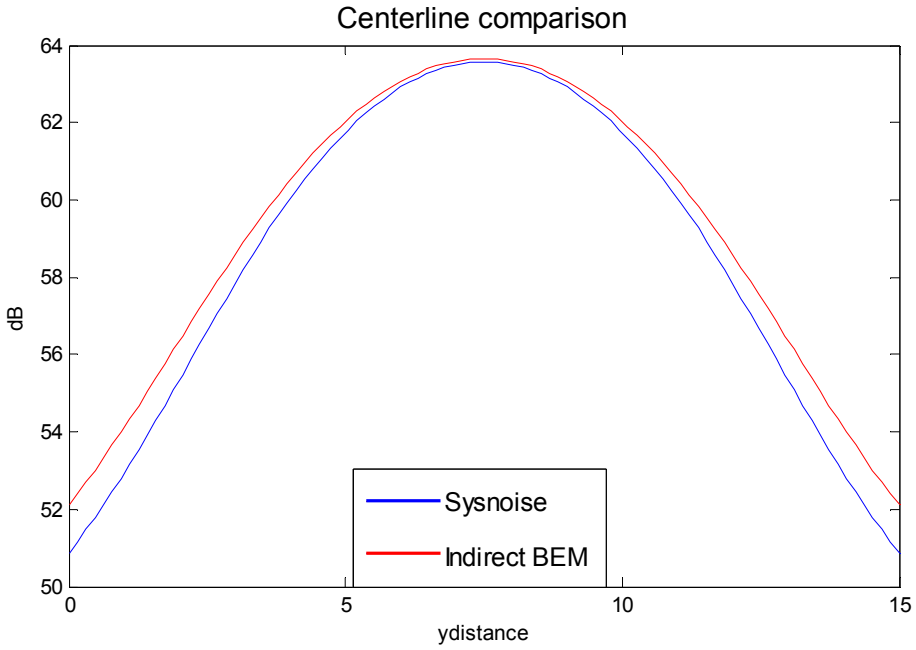

Fig. 5.12 Centerline comparison at 30Hz

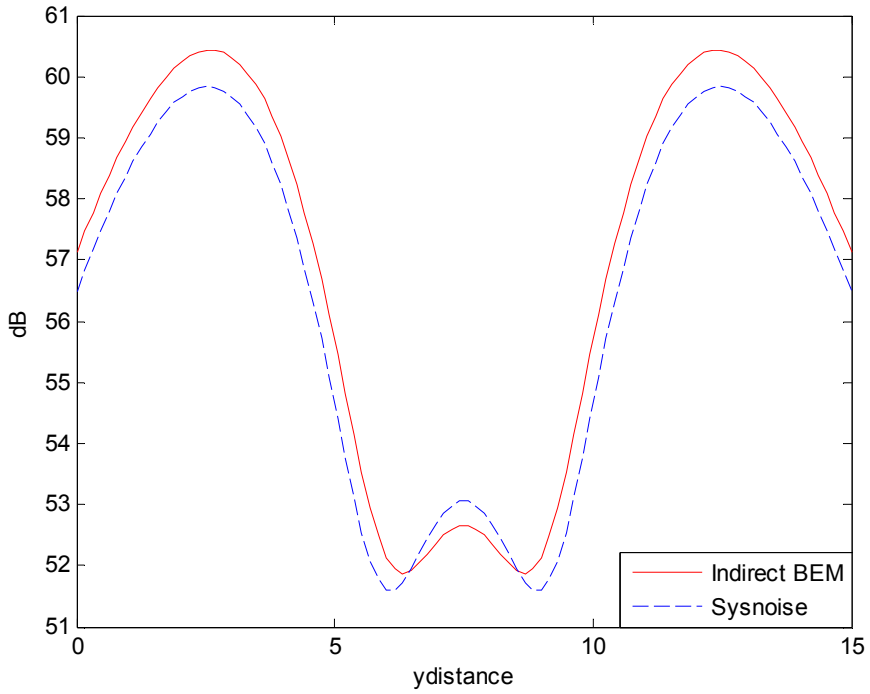

Fig. 5.13 Centerline comparison at 50Hz

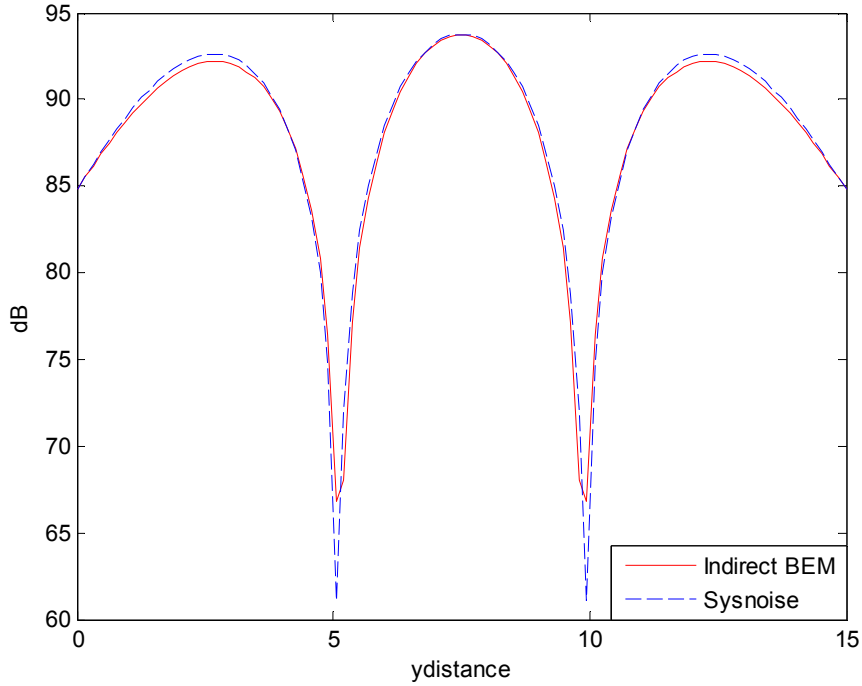

Fig. 5.14 Centerline comparison at 90Hz

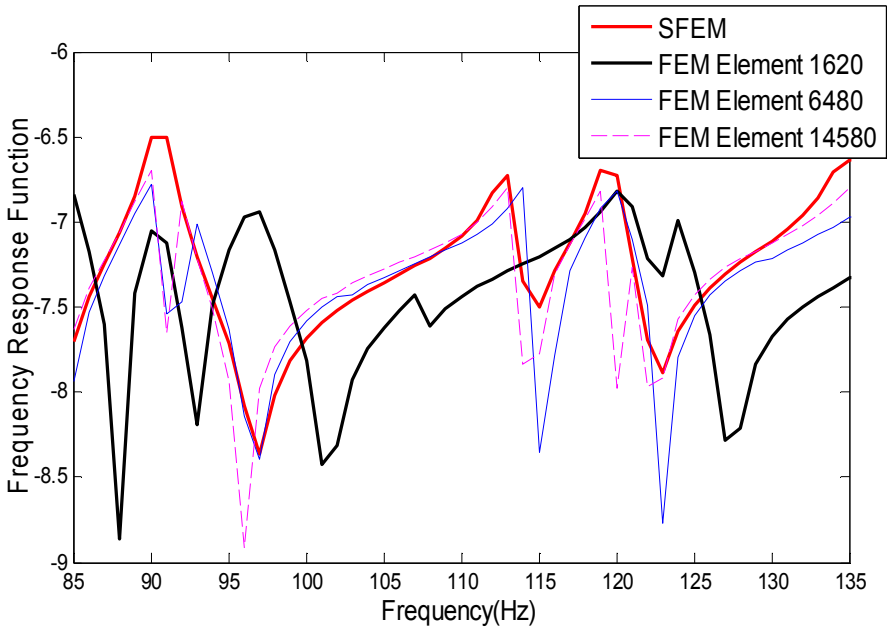

Fig. 5.15 Frequency response function at the frequency range 85Hz ~ 135Hz

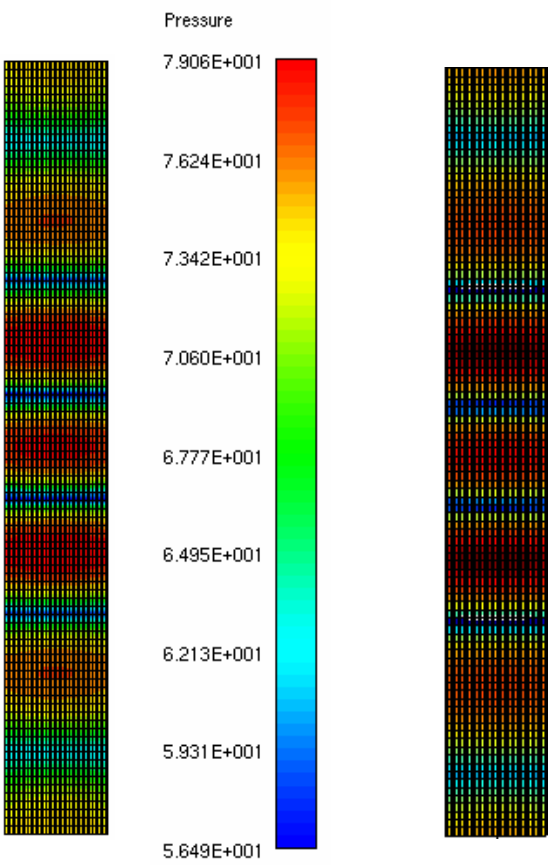

Fig. 5.16 Radiated noise level (dB) at 127Hz:
Matlab coding using indirect BEM (left hand side),
SYSNOISE program (right hand side)

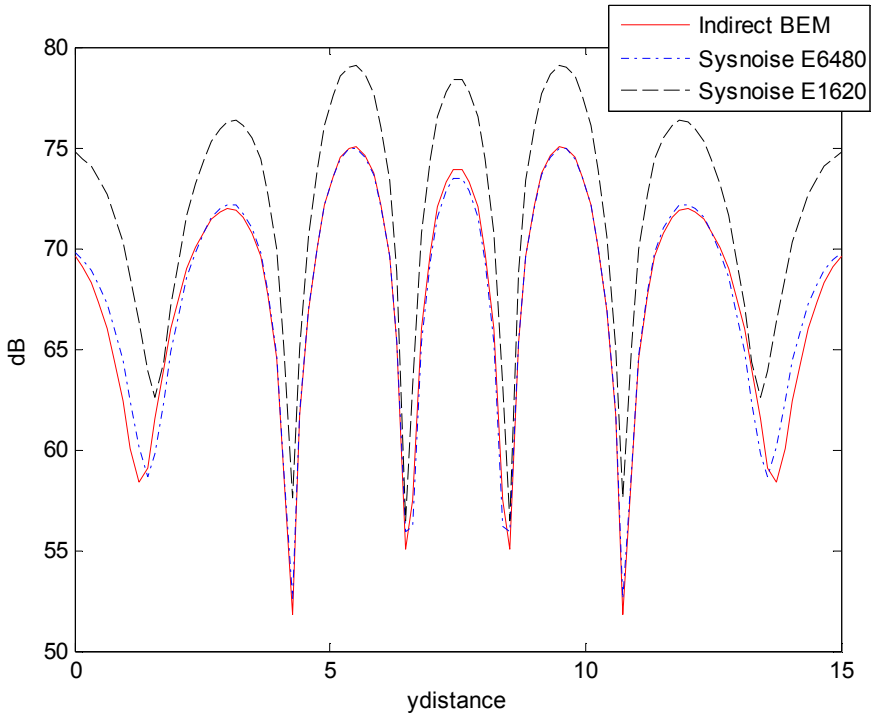

Fig. 5.17 Centerline comparison at 127Hz

Table. 5-1 Properties of the shell model

Property	Value
E	$19.5 \cdot 10^{10}$ (N/m^2)
η	0.01
h	0.01 (m)
ν	0.3
ρ	7700 (kg/m^3)
L	1.57 (m)
W	15 (m)

Table. 5-2 Operation time for the SFEM and the FEM

Classification	Operation time(sec)	$\frac{Operation\ time}{SFEM\ operation\ time}$
SFEM (2 Elements)	373	1
FEM (1620 Elements)	214	0.6
FEM (6480 Elements)	1312	3.5
FEM (14580 Elements)	4117	11.0
FEM (25920 Elements)	8635	23.1

Table. 5-3 Shell model and the field point property

Cylindrical shell model	
Radius	1 (m)
S-directional length	3.14 (m)
Y-directional length	15 (m)
Field	
Points[41(X-dir)×96(Y-dir)]	3936
Transverse length (X-dir)	2 (m)
Longitudinal length (Y-dir)	15 (m)
Height (Z-dir)	5 (m)

6. Conclusion and Recommendations

6.1. Conclusion

In this paper, structural vibration analysis on a circular cylindrical shell was carried out using the spectral finite element method. For formulation with SFEM, first Hamilton's principle was applied to obtain the governing equation of motion of a circular cylindrical shell. Then, using the governing equation of motion, the spectral element matrix that connects nodal displacements and forces is derived. The frequency response functions were obtained from the analysis and compared with the result of NASTRAN, which is commercial tool based on FEM. The comparison showed the reliability of the SFEM formulation on the circular cylindrical shell. With respect to the operation time, SFEM was found to have a huge advantage over FEM in the mid- and high-frequency range.

Radiated noise analysis on a circular cylindrical shell was also carried out. For the analysis, displacements that were obtained from the structural vibration analysis were used as inputs at the boundary. Therefore, one procedure that can analyze both the structural vibration and radiated noise was established. Indirect boundary element method was applied for radiated noise analysis in open sound

field. Results from the analysis were also compared with those from the commercial program, SYSNOISE and the comparison showed well matched results. Moreover, since SFEM gave an almost exact solution, independent of the analysis frequency, the radiated noise analysis using SFEM gives more accurate results than FEM.

6.2. Recommendations

To solve the remaining unsolved problems in this paper, we make two recommendations. First, this research was based on the shallow shell theory, so in the use of Hamilton's principle, the rotational inertia terms were neglected. Researches based on the thick shell theory are recommended. Second, the analysis in this paper was limited to only circular cylindrical shells, so analysis on a general shell is recommended. The governing equation of motion of a general shell will be more complex than that of a circular cylindrical shell, but an analysis of a general shell will be meaningful.

Reference

[1] Usik Lee, 2004, "Spectral Element Method in Structural Dynamics", Inha University Press.

[2] Leissa W., 1973, “Vibration of shells”, Washington DC: US Governing printing office.

[3] Donnell LH., 1938, “A discussion of thin shell theory”, Proceedings of the 5th International Congress of Applied Mechanics.

[4] Lord Rayleigh JWS., 1881, “On the infinitesimal bending of surfaces of revolution.” Proc London Math Soc.

[5] Li Xuebin, 2007, “Study on free vibration analysis of circular cylindrical shells using wave propagation”, Journal of Sound and Vibration 311, 667-682.

[6] X. M. Zhang, G. R. Liu and K. Y. Lam, 2000, “Vibration analysis of thin cylindrical shells using wave propagation approach”, Journal of Sound and Vibration, 239(3), 397-403.

[7] Abhijit Sarkar and Venkata R. Sonti, 2009, “Simplified dispersion curves for circular cylindrical shells using shallow shell theory”, Journal of Sound and Vibration

[8] James F. Doyle, 1997, “Wave propagation in structures”, Springer-Verlag New York, Inc.

[9] C. Wang, J.C.S. Lai, 2000, “Prediction of natural frequencies of finite length circular cylindrical shells”, Applied Acoustics 59 (2000) 385-400.

[10] Stephen P. Timoshenko and S. Woinowky-Krieger, 1959, “Theory of plates and shells”, McGraw-Hill, Inc.

[11] Prem K. Kythe, 1995, “An introduction to boundary element methods”, CRC press, Inc.

[12] Dimitri E BESKOS, 1987, “Boundary element methods in mechanics”, Elsevier Science Publishers B.V.

[13] C. A. Brebbia, 1978, “The boundary element method for engineers.”, Pentech Press.

[14] R. S. Langley, 1993, “A dynamic stiffness/boundary element method for the prediction of interior noise levels”, Journal of Sound and Vibration, 163(2), 207-230.

[15] 송지훈, 2007, “스펙트럴유한요소법을 이용한 감쇠 구조물 해석”, 서울대학교 대학원 공학박사 학위논문.

[16] 주경림, 2006, “복합구조물의 진동해석을 위한 2 차원 스펙트럴유한요소 연구”, 서울대학교 대학원 공학석사 학위논문.

[17] 이성주, 2009, “점탄성층이 삽입된 샌드위치평판의 스펙트럴유한요소해석”, 서울대학교 대학원 공학석사 학위논문

스펙트럴유한요소법과 경계요소법을 이용한 원통형 쉘의 구조진동 및 방사소음 해석

초록

원통형 쉘의 진동 특성은 3차원에 있어서 고려되는 연성효과로 인하여 평판보다 더욱 복잡하다. 원통형 쉘의 운동방정식을 정확하게 그대로 표현하는 것은 어렵고도 복잡한 일이기 때문에, 합리적인 기준을 바탕으로 하여 많은 근사 운동방정식이 제안되어 왔다. 본 연구에서는 단순지지-자유 경계조건을 가지는 원통형 쉘에 대해 주파수응답함수를 도출하기 위해 Love의 가정을 바탕으로 하여 스펙트럴유한요소법을 도입하였다. 일반적으로 시간영역에서 모달해석 방법을 기반으로 하는 유한요소법과는 달리 스펙트럴유한요소법은 지배방정식의 엄밀해로부터 스펙트럴요소행렬을 도출하여 주파수영역에서 해석을 수행하는 방법이라 할 수 있다. 이러한 스펙트럴유한요소법을 이용하여 구조진동 해석하였고, 그 결과의

신뢰성을 검증하기 위해 상용코드인 NASTRAN과의 비교 해석을 수행되었다.

또한, 원통형 쉘의 방사소음 해석을 위해서는 경계요소법이 적용되었다. 경계요소법은 선형 편미분방정식을 풀기 위한 수치적인 해석방법으로 경계에서의 적분 방정식 형태로 나타난다. 특히, 개방된 공간에서의 방사소음 해석을 위하여 간접 경계요소법이 사용되었으며, 구조진동 해석의 변위를 입력값으로 하여 MATLAB 프로그램을 이용, 코드를 작성하였다. 구조진동 해석의 결과값 검증과 마찬가지로, 방사소음 해석의 결과값 검증을 위하여 경계요소법을 기반으로 하는 SYSNOISE와 비교해석 되었다. 이로써, 구조진동과 방사소음을 한번에 해석할 수 있는 절차를 확립하였다.

주요어: 원통형 쉘, 스펙트럴유한요소법, 경계요소법, 주파수응답함수, 구조진동 해석, 방사소음 해석

학번: 2007-22941

Acknowledgment

대학에 입학하고 8년의 세월이 흘렀습니다. 20살의 나이에 상경하여 막연하나마 대학생활의 낭만에 대한 꿈에 부풀어있던 철없었지만 순수했던 그 시절이 떠오릅니다. 지금 돌이켜 보면 8년이라는 세월을 어떻게 보내왔는지 참 신기하기만 합니다. 많은 친구들을 만났고 많은 일들이 있었습니다. 대학에 처음 입학 하던 순간과 마찬가지로 대학원 입학은 대학과 마찬가지로 중대한 시작의 첫걸음이었습니다. 대학원에 처음 입학했을 때의 마음가짐으로 2년을 보내자고 결심했었는데 그게 잘 지켜졌는지, 지금은 잘 모르겠습니다. 아무것도 없었던 책장에는 책들이 그득하게 쌓여있는데, 과연 내 머릿속에도 그만큼 쌓여있을지 확인이라도 할 수 있었으면 좋겠습니다.

하루의 절반이 넘는 시간을 연구실에서 보내게 되다 보니, 연구실은 공부를 하는 곳이기도 했지만, 삶의 일부를 공유하는 공간이기도 했습니다. 매일 같이 공부하고 같이 이야기하고 같이 밥을 먹으면서, 어디 가서도 쉽게 얻을 수 없는 친구들을 만들 수 있었다고 생각합니다.

대학원 생활을 2년 넘게 하면서 더욱 절실히 깨달았던 것은 사람은 혼자서 살기 힘들다는 것입니다. 입학에서부터 졸업까지 제게 도움을 주신 분들이 정말 많습니다. 일단, 연구실 생활을 할 수 있게 해주시고 여러 면으로 도와주신 교수님께 감사의 말씀을 드리고 싶습니다. 연구실에서 배운 많은 것들은 제 삶에 있어서 중요한 것들이었습니다. 그리고 연구실 멤버들에게 한마디씩 남기고 싶네요.

현웅이형: 스타를 잘하시는 현웅이형, 일단 건강한 2세가 태어나길 기원하고(권뚝섬 좋은데요..ㅋ) Post_Doc일이 잘 풀리길 빌어요. 집들이는 아쉽…

화묵이형: 이해심 많은 화묵이형, 태호가 건강하게 잘 크고 박사학위… 파이팅.. '사회생활상담' 감사했습니다.

지훈이형: 코디네이터 지훈이형, 현웅이형이랑 마찬가지로 2세가 건강하게 태어나길 기원하고, 취업잘 하시길…

성희형: 곧 장가가는 성희형, 알아서 잘 하겠지만 가화만사성이라 하잖아 그리고 살 좀 쪄

야지, 그리고 '인생상담도우미'로 임명~ ㅋ
종도: 뭐든 알아서 잘하는 종도, 앞으로도 잘하겠지만 무릎관리 잘하고~ㅋㅋ , 어머니 잘 챙겨드리는 아들되그라~
신웅: 술 잘먹고 밥 잘먹고 잠 잘자는 웅이, 둘레햄 좀 관리해야겠고, 술 쫌 줄이자고. 이것 저것 고마운 내 동기 졸업 파이팅이다~
주범: 닭가슴살 쭈쭈루, 머 별일이야 있겠냐만은, 지은이랑 잘 지내고 운동 열심히 하그라 그러면 졸업이 보일것이니 ㅋㅋ
경현: 수학 신동 경현이, 넌 너무 수학에 몰입해 있어 ㅋ, 그리고 '의' 발음 고치고, 농구 적당히 해라, 욕도 알지?
이수: 언제나 앞서가는 이수, 게임도 정보도 인생도 한걸음 앞에서 나아가는 이수, 박사 잘 하리라 본다. 우리 온라인에서 함께 하자 ㅋ
재욱: 말 많은 재욱이, 넌 말로 살풀이 하는 거 같다. 후딱 여자친구 만들어라.. 형도 알지? 위로도 잘하지만, 도발도 잘하는 건 뭐다? ㅋㅋ
성원: 야구 신동 성원, 잘은 모르겠다만 카드가 괜찮더구나, 앞으로 연구실 생활 잘하고 힘들면 재욱이한테 상담을…
준수: 뭐든 열심히 하는 준수, 처음 들어올 때 이미지와는 다르게 열심히 하는 모습 보기 좋고, 나도 드라마가 좋아~ , 연구실 생활 잘 하고

그리고 제 곁에서 기쁠 때나 슬플 때나 함께 해준 4총사 「재균」,「성우」,「순재」, 친근하게 연락하는 후배 「광의」, 의리 있는 치과의사 '「재영」, 조선소에 가있는 「성주」, 대전 패밀리 「영훈」,「강석」,「신하」,「현제」,「창용」 에게 고맙다고 사랑한다고 전하고 싶습니다.

마지막으로 스물 여덜이 될 때까지 저를 키워주시고 항상 사랑해 주시는 우리 어머니, 아버지, 그리고 누나에게 깊은 감사의 마음을 전하고 싶습니다. 언제나 가족은 저에게 있어서 삶을 살아가는 원동력이자 제가 지키고 사랑해야 할 보금자리였습니다. 사랑합니다.

P.S. 여름 햇살이 타오를 듯 비치는 지금 이곳 관악 캠퍼스는 언제나 서울 평균 기온을 기준으로 1~2도쯤은 낮은 기온을 형성합니다. 전망이 좋을

때는 저기 멀리 서울타워가 보이고요. 여의도에서 불꽃 축제를 하면 학교에서 소리가 들릴 정도로 가까운 곳에 위치하고 있습니다. 학교 바로 옆에 있는 계곡은 비가 많이 온 다음날이면 시원한 장면을 연출합니다. 또한 까치가 날아다니고, 장끼가 출몰하기도 하며, 다람쥐와 고양이들이 활보하기도 하죠. 주말에는 등산객들과 버들골로 놀러 나온 피서객들이 가득 메우는 곳입니다. 눈이 많이 오면 제설작업에 특별히 신경 써야 하는 곳이며, 비가 오는 날이면 자면서 개구리 울음소리를 들을 수 있는 곳이죠.

상경함과 동시에 살게 된 이곳 관악캠퍼스에서의 8년 반의 세월은 제 고향인 대전의 어느 장소보다도 이곳을 더 친숙하게 만들어 버렸습니다. 너무나 자연스럽고 당연하게 받아들인 이곳에서의 생활은 머물 날이 얼마 남지 않은 지금 생각해 보면 저에게 있어서 큰 축복이었음을 깨닫게 됩니다. 이 곳이 그리워지겠지만, 아름다운 추억으로 간직할 수 있다는 마음가짐으로 펜을 놓고자 합니다.

2009년 8월
관악캠퍼스에서